Molecular Pharmacology Fast Forward. Published on February 26, 2016 as DOI: 10.1124/mol.116.103697
This article has not been copyedited and formatted. The final version may differ from this version.

MOL#103697

All-trans-retinoic acid Enhances Mitochondrial Function in Models of Human Liver

Sasmita Tripathy, John D Chapman, Chang Y Han, Cathryn A Hogarth, Samuel L.M. Arnold, Jennifer Onken, Travis Kent, David R Goodlett and Nina Isoherranen

Departments of Pharmaceutics (ST, SLA, NI), Medicinal Chemistry (JDC, DRG), and Diabetes Obesity Center for Excellence and the Department of Medicine, Division of Metabolism, Endocrinology and Nutrition (CYH), University of Washington, Seattle, WA; School of Molecular Biosciences and The Center for Reproductive Biology, Washington State University, Pullman, WA (CAH, JO, TK); School of Pharmacy, University of Maryland, Baltimore, MD (DRG)

Molecular Pharmacology Fast Forward. Published on February 26, 2016 as DOI: 10.1124/mol.116.103697
This article has not been copyedited and formatted. The final version may differ from this version.

Running Title: Retinoic acid increases fatty acid β-oxidation

Corresponding Author: Nina Isoherranen, Department of Pharmaceutics, School of Pharmacy, University of Washington, Health Science Building, Room H-272M, Box 357610, Seattle, Washington 98195-7610 USA, Phone: 206-543-2517; Fax: 206-543-3204; Email: ni2@uw.edu

Text Pages: 27

Figures: 9

References: 26

Words in Abstract: 248

Words in Introduction: 750

Words in Discussion: 1461

Abbreviations:

*at*RA, All-trans retinoic acid; RAR, Retinoic acid receptor; PPAR, Peroxisome proliferator activated receptor; SHP, Small heterodimer partner; ALDH1A, Aldehyde dehydrogenase 1; CPT1α, Carnitine palmitoyltransferase 1α; FGF21, Fibroblast growth factor 21; NAFLD, Non-alcoholic fatty liver disease; PGC1α, Peroxisome proliferator activated receptor gamma coactivator 1α; PGC1β, Peroxisome proliferator activated receptor gamma coactivator 1β; NRF1, Nuclear respiratory factor 1; ACSL, Acyl CoA synthase ligase; ACAD, Fatty acyl CoA dehydrogenase; ECH1, Enoyl CoA hydratase 1; IDH2, Isocitrate dehydrogenase; ATP5A1, ATP synthase subunit α; ATGL, Adipose triglyceride lipase; SREBP1, Sterol regulatory element binding protein 1; DGAT2, Diacylglycerol O-acyl transferase 2; MTTP, Microsomal triglyceride transfer protein; FASN, Fatty acid synthase; SDHA, succinate dehydrogenase subunit A; SD, standard deviation.

Molecular Pharmacology Fast Forward. Published on February 26, 2016 as DOI: 10.1124/mol.116.103697
This article has not been copyedited and formatted. The final version may differ from this version.

ABSTRACT

All-trans-retinoic acid (*at*RA) is the active metabolite of vitamin A. The liver is the main storage organ of vitamin A, but activation of the retinoic acid receptors (RARs) in mouse liver and in human liver cell lines has also been shown. While *at*RA treatment improves mitochondrial function in skeletal muscle in rodents, its role in modulating mitochondrial function in the liver is controversial, and little data is available regarding the human liver. The aim of this study was to determine whether *at*RA regulates hepatic mitochondrial activity. *at*RA treatment increased the mRNA and protein expression of multiple components of mitochondrial β-oxidation, TCA cycle and respiratory chain. Additionally, *at*RA increased mitochondrial biogenesis in human hepatocytes and in HepG2 cells with and without lipid loading based on PGC1α, PGC1β and NRF1 mRNA and mitochondrial DNA quantification. *at*RA also increased β-oxidation and ATP production in HepG2 cells and in human hepatocytes. Knockdown studies of RARα, RARβ and PPARδ revealed that the enhancement of mitochondrial biogenesis and β-oxidation by *at*RA requires PPARδ. In vivo in mice, *at*RA treatment increased mitochondrial biogenesis markers after an overnight fast. Inhibition of *at*RA metabolism by talarozole, a CYP26 specific inhibitor, increased the effects of *at*RA on mitochondrial biogenesis markers in HepG2 cells and in vivo in mice. These studies show that *at*RA regulates mitochondrial function and lipid metabolism, and that increasing *at*RA concentrations in human liver via CYP26 inhibition may increase mitochondrial biogenesis and fatty acid β-oxidation, and provide therapeutic benefit in diseases associated with mitochondrial dysfunction.

Molecular Pharmacology Fast Forward. Published on February 26, 2016 as DOI: 10.1124/mol.116.103697
This article has not been copyedited and formatted. The final version may differ from this version.

Introduction

Vitamin A (retinol) is stored predominantly in the liver as retinyl esters. However, the active metabolite of retinol, *all-trans*-retinoic acid *(at*RA), appears to also regulate gene transcription in the liver (O'Byrne and Blaner, 2013). Most actions of *at*RA are mediated via interactions with retinoic acid receptors (RARs) (Wolf, 2010; Yu et al., 2012), but *at*RA also activates the peroxisome proliferator-activated receptor (PPAR)-β/δ (Berry and Noy, 2007; Shaw et al., 2003; Wolf, 2010). In addition, *at*RA induces the expression of the transcriptional repressor small heterodimer partner (SHP) in the liver resulting in broad effects on gene transcription, especially of genes responsible for bile acid metabolism and transport (Koh et al., 2014; Mamoon et al., 2014; Yang et al., 2014). The activation of multiple pathways by *at*RA likely leads to diverse effects on liver physiology including altered lipid homeostasis. In humans both excessive intake of vitamin A or retinoids and vitamin A deficiency lead to hypertriglyceridemia, elevated total cholesterol and decreased HDL-cholesterol (Bershad et al., 1985; Brelsford and Beute, 2008; Lawrence et al., 2001; Lilley et al., 2013; Staels, 2001). However, likely due to a dichotomy of the effects of vitamin A on the liver, the endogenous role of *at*RA in regulating lipid and fatty acid homeostasis and role of *at*RA in liver disease is not well understood.

In rodents *at*RA appears to regulate various processes in lipid homeostasis in a species specific manner. Data from several mouse studies suggest that *at*RA signaling via RAR is needed to maintain liver mitochondrial fatty acid oxidation and lipid homeostasis. Hepatocyte specific RAR knock-out mice develop microvesicular steatosis, hepatocellular carcinoma, decreased mitochondrial fatty acid oxidation and increased peroxisomal and microsomal fatty acid oxidation presumably due to deficient *at*RA signaling (Yanagitani et al., 2004). Similarly, in normal mice *at*RA enhances fatty acid oxidation and ketogenesis via RAR activation and FGF21

Molecular Pharmacology Fast Forward. Published on February 26, 2016 as DOI: 10.1124/mol.116.103697
This article has not been copyedited and formatted. The final version may differ from this version.

induction (Amengual et al., 2012; Li et al., 2013). In agreement with a role of *at*RA in maintaining lipid homeostasis in the liver, decrease of hepatic *at*RA concentrations via inhibition of *at*RA synthesis in mice led to microvesicular vacuolation but without a change in liver triglycerides (Paik et al., 2014). However, in diet induced obese mice *at*RA treatment decreased hepatic triglyceride content (Berry and Noy, 2009) and hepatic lipid accumulation (Kim et al., 2014). In contrast, in rats vitamin A deficiency led to increased expression of genes involved in fatty acid metabolism in the liver (McClintick et al., 2006) and decreased liver total phospholipid content and phosphatidylcholine synthesis (Oliveros et al., 2007), demonstrating opposite effects to those observed in mice. Low retinol diet also significantly decreased stellate cell free fatty acids and total lipids while high retinol diet increased triglycerides, cholesteryl esters, free fatty acids and total lipids in rat stellate cells (Moriwaki et al., 1988). How well these observations in mice or rats reflect *at*RA signaling in healthy or diseased human liver is not known.

Hepatic vitamin A stores are depleted in alcoholic liver disease, and vitamin A deficiency is believed to play a role in the development and progression of the disease (Bell et al., 1989; Clugston et al., 2013; Lee and Jeong, 2012; Ward and Peters, 1992). Current data also strongly suggests that altered vitamin A homeostasis and retinoid metabolism is present in nonalcoholic fatty liver disease (NAFLD) and in subsequent steatosis. In liver biopsies from patients with NAFLD, the mRNA of retinaldehyde dehydrogenases involved in *at*RA formation, and the mRNA of CYP26A1 responsible for *at*RA metabolism was increased (Ashla et al., 2010). In addition, in a panel of human livers with increasing level of steatosis, retinol and retinyl ester concentrations and RARβ mRNA decreased significantly with increasing steatosis (Trasino et al., 2015). Finally, in a study of patients with NAFLD and steatosis, RA concentrations were significantly lower in plasma from patients than in healthy controls (Liu et al., 2015). Yet,

Molecular Pharmacology Fast Forward. Published on February 26, 2016 as DOI: 10.1124/mol.116.103697
This article has not been copyedited and formatted. The final version may differ from this version.

detailed studies of retinoid signaling in models of NAFLD have not been conducted. As NAFLD is at least in part a mitochondrial disease associated with decreased mitochondrial gene expression and function (Aharoni-Simon et al., 2011; Betancourt et al., 2014; Pessayre, 2007; Wei et al., 2008), regulation of mitochondrial fatty acid oxidation and lipid homeostasis by *at*RA could play a role in NAFLD progression. The aim of this study was to determine whether *at*RA regulates mitochondrial function and lipid homeostasis in the healthy and fatty human liver and to establish how well mouse and rat models of *at*RA signaling in the liver correlate with findings of *at*RA signaling in models of human liver.

Materials and Methods

Chemicals and Reagents: Dulbecco's modified essential medium (DMEM) with high glucose (25 mM) and fetal calf serum were obtained from Invitrogen. All-*trans*-retinoic acid (*at*RA) was obtained from Sigma-Aldrich, St. Louis, MO. GW0742 (PPARδ agonist) and TTNPB (RARs pan agonist) were obtained from Tocris, Minneapolis, MN. Talarozole (R115866) was obtained from MedChem Express, Princeton, NJ. siRNAs for RARα, RARβ and PPARδ were obtained from Ambion, Life Science Technologies, Grand Island, NY. ATP assay kit was purchased from Biovision Inc., Milpitas, CA. Human primer and probe pairs such as PGC1α (Hs01016719_m1, FAM), PGC1β (Hs00991677_m1, FAM), NRF1 (Hs00192316_m1, FAM), CPT1α (Hs00912671_m1, FAM), PPARα (Hs00947536_m1, FAM), PPARδ (Hs04187066_g1, FAM), PPARγ (Hs01115513_m1, FAM), GAPDH (Hs99999905_m1, VIC), RARα (Hs00940446_m1, FAM), RARβ (Hs00233407_m1, FAM), ATGL (Hs00386101_m1, FAM), DGAT2 (Hs01045913_m1, FAM), MTTP (Hs00165177_m1, FAM) and SREBP1 (Hs01088691_m1, FAM) were obtained from Applied Biosystems, Carlsbad, CA. Mouse primer

Molecular Pharmacology Fast Forward. Published on February 26, 2016 as DOI: 10.1124/mol.116.103697
This article has not been copyedited and formatted. The final version may differ from this version.

and probe pairs including Rarβ (Mm01319677_m1, FAM), Cyp26a1 (Mm00514486_m1, FAM), Pgc1α (Mm01208835_m1, FAM), Cpt1α (Mm01231183_m1, FAM), Atgl (Mm00503040_m1, FAM), Pgc1β (Mm00504720_m1), Nrf1 (Mm01135606_m1) and β-Actin (Mm00607939_s1, FAM) were obtained from Applied Biosystems, Carlsbad, CA. Mitochondrial genes and nuclear gene primers set #7246 (for human) and #RR290 (for mouse) were purchased from Takara Clontech, Mountain View, CA.

HepG2 cell culture: HepG2 cells were cultured in 6-well plates (Corning Life Sciences, Corning, NY) with a cell density $1x10^6$ cells per well in DMEM with 25 mM glucose media with 10% fetal calf serum in a 5% carbon dioxide environment in a humidified incubator at 37 °C. All media contained penicillin and streptomycin and all the studies were conducted in triplicate. Lipid loaded HepG2 cells were used as a model for fatty liver. For lipid loading, HepG2 cells were treated with 200 μM oleic acid for 3 days. Every 24 hours 200 μM oleic acid was added to the media. The lipid loading was confirmed by Oil Red O staining (BioVision Inc, Milpitas, CA) according to manufacturer's recommendations.

Cell viability assay: HepG2 cell growth was measured using WST-1 reagent (Roche, Indianapolis, IN, USA). Briefly, cells were grown in a 96 well plate cultured in a 5% carbon dioxide environment in a humidified incubator at 37 °C. Using 6 replicates per treatment and a 0.1% DMSO control, the effect of *at*RA treatment (0.001 – 50 μM) on cell proliferation was measured after 72 hours of treatment. Every 24 hours, the media was removed, cells were washed with PBS, and the media containing *at*RA was replaced in order to maintain constant *at*RA concentrations. At 72 hours, 10 μL of WST-1 reagent was added to each well and incubated at 37 °C for 1 hour to measure cell viability and growth according to manufacturer's instructions. The absorbance was measured at 450 nm with background subtraction at 680 nm.

Molecular Pharmacology Fast Forward. Published on February 26, 2016 as DOI: 10.1124/mol.116.103697
This article has not been copyedited and formatted. The final version may differ from this version.

Each treatment was normalized to the control cells and cell viability was expressed as a percentage of the control.

Human hepatocyte experiments: Cryopreserved human hepatocytes from five donors (3 females and 2 males aged 13-52 years) were obtained from Xenotech (Lenexa, KS). Hepatocytes were thawed at 37°C, placed into thawing media (K2000; Xenotech, Lenexa, KS) and cell viability was confirmed using trypan blue. Hepatocytes were diluted in plating media (Williams E media plus hepatocytes supplement pack CM3000, LifeTechnologies, Grand Island, NY) at $1.2x10^6$ live cells. 330 μl of plating media containing hepatocytes were added to each well in 12 or 24-well collagen type-I coated plates (LifeTechnologies, Grand Island, NY) and allowed to attach for ~8 hours. The plating media was then replaced with Williams E media containing cell maintenance supplements (CM4000; LifeTechnologies, Grand Island, NY). Hepatocytes from 3 donors were plated and treated with 1 μM *at*RA or ethanol as a vehicle control for 24 hours and at the end of the 24 hour treatment, cells were harvested for PGC1α, PGC1β and NRF1 mRNA measurements or for quantification of ATP production or mitochondrial DNA quantification. Hepatocytes were treated with 1 μM *at*RA or ethanol as a vehicle control for 48 hours for SDHA protein quantification. For lipid loading, human hepatocytes were loaded with 600 μM oleic acid once for 24 hours and then treated with 1 μM *at*RA or ethanol as a vehicle control for 24 hours. At the end of the 24 hour treatment, the cells were harvested for PGC1α, PGC1β and NRF1 mRNA measurements or analyzed for ATP production. All treatments were conducted in triplicate.

Proteomic Analysis: Proteomic changes driven by *at*RA in HepG2 cells were evaluated using the PAcIFIC shotgun proteomic method (Chapman et al., 2015). HepG2 cells were treated with either *at*RA (10 μM) or 0.1% DMSO (vehicle control) for 72 hours and harvested. For

Molecular Pharmacology Fast Forward. Published on February 26, 2016 as DOI: 10.1124/mol.116.103697
This article has not been copyedited and formatted. The final version may differ from this version.

proteomic analysis HepG2 cells were cultured in DMEM media supplemented with 10% FBS and 1% penicillin/streptomycin in 10 cm^2 dishes and cells were grown to 70% confluence. The cells were treated with either *at*RA (10 μM) or 0.1% DMSO (control) for 72 hours. The media was replaced every 24 hours with fresh treatment media containing either *at*RA or DMSO till harvest. Cells were harvested by washing them twice with ice cold PBS and scraping the cells into 0.5 mL of 100 mM ammonium bicarbonate for shotgun proteomics analysis. Harvested cell suspension was sonicated to lyse the cells and subsequently centrifuged at 5,000 g to pellet cellular debris. Supernatant from each sample was collected and placed in a clean eppendorf tube on ice. Protein quantification was performed with a BCA protein quantification kit following the manufacturer's protocol (Thermo Scientific, Waltham, MA). Protein quantity was normalized for each sample prior to further proteomics sample preparation. The samples with 200 μg protein per 100 μL were denatured with the addition of 6 M urea. Subsequently, samples were buffered with the addition of 7 μL 1.5 M Tris pH 8.8, reduced with 2.5 μL of 200 mM tris-2-carboxyethyl phosphine (TCEP) for 1 hour at 37 °C, alkylated with 20 μL of 200 mM iodoacetamide for 1 hour at room temperature in the dark, and then quenched with 20 μL of 200 mM dithiothreitol. Prior to addition of sequencing-grade porcine trypsin (Promega, Madison, WI, USA) at a protein to enzyme ratio of 50:1, samples were diluted with 900 μL of 50 mM ammonium bicarbonate and 200 μL of MeOH. After an overnight incubation, peptides were desalted on a Vydac C18 macrospin column (The Nest Group, Southborough, MA, USA) according to the manufacturer's protocol. Resulting eluent was concentrated on a SPD 111V SpeedVac (Thermo Savant, San Jose, CA, USA) and stored until further use. Peptide digests were analyzed on an LTQ Oribtrap (Thermo Fisher, San Jose, CA, USA) coupled with a nano-electrospray ionization in positive ion mode. For the PAcIFIC acquisition, Captive spray ionization (CSI) mass spectrometry was

Molecular Pharmacology Fast Forward. Published on February 26, 2016 as DOI: 10.1124/mol.116.103697
This article has not been copyedited and formatted. The final version may differ from this version.

performed using a Waters NanoAquity (Milford, MA, USA). The mass spectrometer parameters were set as defined previously (Panchaud et al., 2011; Panchaud et al., 2009). A fused silica 200 μm ID trapping column purchased from New Objective (Woburn, MA, USA) and packed with 2 cm of 200 Å, 5 μm Magic C18AQ particles (Michrom, Auburn, CA, USA) was used. Successive analytical separation was performed on a fused silica 200 μm ID trapping column purchased from New Objective (Woburn, MA, USA) and packed with 15cm of 100 Å, 5 μm Magic C18AQ particles (Michrom, Auburn, CA, USA). For each sample injection, 1 μg of the peptide sample was loaded on the trapping column at 6 μL/min with 95% water/5% acetonitrile/0.1% formic acid for 2.5 minutes. Trapped peptides were then eluted from the trapping column onto the analytical column using a variable gradient with a flow rate of 2.5 μL/min. The gradient utilized two mobile phase solutions: A, water/0.1% formic acid; and B, acetonitrile/0.1% formic acid. For MS, ion source conditions were optimized using the tuning and calibration solution suggested by the instrument manufacturer and under conditions recommended by the CSI manufacturer (Bruker/Michrom). Data acquired was converted from Thermo's RAW format to the universal mzXML format and searched against the IPI human database v3.49 (http://www.ebi.ac.uk/IPI/IPIhuman.html) using SEQUEST (Havilio et al., 2003). The precursor ion tolerance was set to 3.75 and additional search parameters for SEQUEST included trypsin enzyme specificity, cysteines modified with iodoacetamide and the variable option for methionines in reduced or oxidized form. Results were analyzed with Peptide Prophet (Keller et al., 2002; Nesvizhskii et al., 2003) ensuring that peptide hits with a probability of >0.99 were accepted and linked to protein entries. Protein identifications were assigned relative quantification values using in-house spectral counting software (Ryu et al., 2008). The relative quantification value for each protein is determined by summing all peptide tandem MS spectra

Molecular Pharmacology Fast Forward. Published on February 26, 2016 as DOI: 10.1124/mol.116.103697
This article has not been copyedited and formatted. The final version may differ from this version.

correlated to a respective protein (Liu et al., 2004). Following spectral counting, the data was filtered using a Student's t-test and a p-value cutoff of 0.05 to ensure that protein changes were consistent throughout the biological triplicate and technical duplicate analyses.

mRNA analysis and quantitative RT-PCR: RT-PCR was used to quantify mRNA expression of various genes (StepOnePlus^{TM}, Applied Biosystems, Carlsbad, CA) as previously described (Tay et al., 2010). For mRNA extraction, 300 µl of TRI reagent (Invitrogen, Grand Island, NY) was added to each well containing cultured HepG2 cells or hepatocytes after aspiration of all media and mRNA extracted according to the manufacturer's recommendations. Total RNA was quantified using the Nanodrop 2000c Spectrophotometer (Thermofisher Sci., Waltham, MA). cDNA was synthesized from 1 µg mRNA using TaqMan® Gene expression reagents (Applied Biosystems, Carlsbad, CA). TaqMan real-time gene expression master mix and PCR primers and fluorescent probes were obtained from Applied Biosystems (Foster City, CA). Probes were labeled with the 5'-reporter dye 5-carboxyfluorescein and a nonfluorescent black hole quencher on the 3'-end. GAPDH was used as the housekeeping gene and all assays were done as multiplexes. No changes in GAPDH mRNA levels were observed in any of the experiments. All biological triplicate samples were analyzed in duplicate. Changes in target mRNA were measured using relative quantification (fold-difference) and the $\Delta\Delta C_T$ method (Tay et al., 2010).

Effects of *at*RA on mitochondrial number, function and protein expression: The effect of *at*RA on mitochondrial number, function and protein expression was determined by measuring ATP production, fatty acid oxidation, quantity of mitochondrial DNA and expression of succinate dehydrogenase subunit A (SDHA). All experiments were conducted as biological triplicates.

Molecular Pharmacology Fast Forward. Published on February 26, 2016 as DOI: 10.1124/mol.116.103697
This article has not been copyedited and formatted. The final version may differ from this version.

For western blotting proteins were extracted as whole cell extract from HepG2 cells treated with vehicle (ethanol) or 1 μM *at*RA for 48 hours using whole cell lysis buffer in the presence of protease (Roche Applied Science, Indianapolis, IN) and phosphatase inhibitors (1 mM β-glycerol phosphate, 2.5 mM Na-pyrophosphate, 1 mM Na_3VO_4). Protein concentrations were measured by BCA protein assay. Whole cell protein extracts were separated by SDS-polyacrylamide gel electrophoresis (NuPAGE-Novex 4–12% polyacrylamide Bis-Tris, Life Science Technologies) and transferred to nitrocellulose membranes. Blots were incubated with primary antibodies against SDHA and β-actin overnight at 4°C. Next day blots were washed and incubated with secondary antibody for one hour at room temperature. Antigen-antibody reactions were detected and quantified using LiCor Odyssey scanner and software (Licor Inc., Lincoln, NE). SDHA (product#5839) was purchased from Cell Signaling, Danvers, MA. β-Actin antibody (product#AC-15) was obtained from Abcam, Cambridge, MA. The secondary antibodies, IRDye 680 (antimouse; product#925-68070) and IRDye 800, (anti-rabbit; product#925-32211) were obtained from LiCor, Inc., Lincoln, NE. All western blots were conducted as technical duplicates.

To measure β-oxidation, [1-^{14}C] palmitate (American Radiolabeled Chemicals Inc) was used. HepG2 cells were gently detached with non-enzymatic dissociation solution (Sigma), and suspended in Krebs-Ringer buffer containing 1 nM insulin and placed in vials. Wells containing cylinders of Whatman filter paper were suspended above the HepG2 cells containing solution in vials. The vials were stoppered with rubber caps, gassed with 95% O_2-5% CO_2, and 0.5 μCi of [1-^{14}C] palmitate for β-oxidation were injected into the vials. After incubation for 3 hrs at 37 ^{o}C, 200 μl hyamine hydroxide was injected into the wells containing the filter paper, 200 μl of 1N

Molecular Pharmacology Fast Forward. Published on February 26, 2016 as DOI: 10.1124/mol.116.103697
This article has not been copyedited and formatted. The final version may differ from this version.

HCl was added to the HepG2 cells, and the vials were incubated overnight at 37 ^{o}C. The filter paper in the wells was then transferred to 10 ml of scintillation fluid and counted.

To measure ATP production, 10^5 HepG2 cells per well were plated in a 12-well plate. HepG2 cells were treated with 0.01-10 μM *at*RA for 24 hours. Cells were then harvested for the ATP assay and ATP was quantified from the cell lysate using a commercially available colorimetric kit purchased from Biovision Inc., Milpitas, CA. Total ATP production was normalized to milligram protein. For ATP assay in normal and lipid loaded human hepatocytes, hepatocytes were treated with 1 μM *at*RA for 24 hours and then cells were harvested for the ATP assay as described above.

To quantify mitochondria number, the mitochondrial DNA was quantified using qPCR. Genomic DNA from HepG2 cells and human hepatocytes was extracted by using DNAzol. Total DNA was quantified using the Nanodrop 2000c Spectrophotometer (Thermofisher Sci., Waltham, MA). 100 ng genomic DNA per reaction was used to perform qPCR. The mitochondrial and nuclear genes primer set were obtained from Takara Clontech, Mountain View, CA. No changes in nuclear DNA levels were observed in any of the experiments. All biological triplicate samples were analyzed in duplicate. Changes in mitochondrial DNA copy number was measured using relative quantification (copy number) versus nuclear DNA and the $\Delta\Delta C_T$ method.

Role of RAR and PPARδ on RA signaling in the liver: To determine the nuclear receptors potentially responsible for *at*RA effects on mitochondrial function, HepG2 cells were first treated with 1 μM *at*RA, 50 nM TTNPB (RAR pan agonist) or 200 nM GW0742 (PPARδ agonist) or vehicle (ethanol) for 24 hours and the mRNA expression of PGC1α, PGC1β and NRF1 was measured using RT-PCR as described above. Second RARα, RARβ and PPARδ

Molecular Pharmacology Fast Forward. Published on February 26, 2016 as DOI: 10.1124/mol.116.103697
This article has not been copyedited and formatted. The final version may differ from this version.

siRNA was used in normal and lipid loaded HepG2 cells together with 1 μM *at*RA or vehicle treatment for 48-72 hours to determine the effects of each nuclear receptor knock down on PGC1α, PGC1β and NRF1 mRNA and on ATP production, SDHA protein content, mitochondrial number and β-oxidation. siRNA for RARα (s11801), RARβ (s11803) and PPARδ (s10883) were purchased from Ambion, ThermoFisher Scientific, Waltham, MA. Lipofectamine RNAiMAX transfection reagent (13778-075) was purchased from Invitrogen, ThermoFisher Scientific, Waltham, MA. For the siRNA experiments 10^6 HepG2 cells were grown in 6 well plates as described above. Cells were transfected with either siRNA for RARα, RARβ and PPARδ or control siRNA (scrambled RNA) at 25 pmol/well together with 7.5 μl/well of the lipofectamine RNAiMAX transfection reagent according to the manufacturer's recommendations. 48 hours after the transfection, 1 μM *at*RA or vehicle was added to the media. After 24 hours of *at*RA treatment, cells were harvested, and either RNA extracted and the expression of PGC1α, PGC1β and NRF1 was measured or ATP production, SDHA protein, β-oxidation or mitochondrial number were measured as described above. The knock down of PPARδ and RARβ was confirmed by western blot of PPARδ and RARβ protein expression. Antibodies for PPARδ (ab137724) and RARβ (EPR2017) were purchased from Epitomics-Abcam, Cambridge, MA. Western blotting was conducted as described above using whole cell lysate.

Effect of CYP26 inhibition on *at*RA potency: Normal and lipid loaded HepG2 cells were treated with 1 μM *at*RA or ethanol (vehicle) in the presence and absence of 1 μM talarozole (a CYP26 specific inhibitor) for 24 hours. Media was collected for *at*RA and *at*RA metabolite (4-OH-*at*RA and 4-oxo-*at*RA) analysis by LC-MS/MS as previously described (Topletz et al., 2015) using an AB Sciex QTRAP 4500 mass spectrometer operated on a negative ion

Molecular Pharmacology Fast Forward. Published on February 26, 2016 as DOI: 10.1124/mol.116.103697
This article has not been copyedited and formatted. The final version may differ from this version.

electrospray detection and coupled with an LC-20AD® ultra fast liquid chromatography (UFLC) system (Shimadzu Co., Kyoto, Japan) and Agilent Zorbax C18 column (3.5 μm, 2.1 mm x 100 mm). Cells were harvested for RNA extraction and mRNA expression of PGC1α, PGC1β and NRF1 was measured as described above. In a separate study, HepG2 cells were treated with 1 μM *at*RA or ethanol (vehicle) in the presence and absence of 1 μM talarozole for 24 hours and ATP production was measured as described above.

Effect of RA and Talarozole (TLZ) treatment on mitochondrial biogenesis in mice: All animal experiments were approved by Washington State University Animal Care and Use Committee and were conducted in accordance with the guiding principles for the care and use of research animals of the National Institutes of Health. Mixed background (129/C57BL/6) mice housed in a temperature- and humidity-controlled environment with food and water provided ad libitum were used for the studies. Prior to tissue collection, the animals were euthanized by CO_2 asphyxiation, followed by cervical dislocation, and livers removed and snap frozen in light-protected tubes until analysis.

To determine the effect of *at*RA treatment on mitochondrial biogenesis in mice, young adult (~60 dpp) female mice were treated once daily i.p. with 5 mg/kg *at*RA (Sigma Aldrich, St. Louis, MO, USA) dissolved in 15% DMSO/85% sesame oil or vehicle for five consecutive days. Twelve hours after the final dose, all food was removed and all mice were fasted for 12 hours. Following the fast, the mice were split into fasted and refed treatment groups. Animals in the fasted group were euthanized and livers collected 24 hours following the final RA or vehicle control dose, immediately following the 12 hour fast. For the refed group, food was added to cages after the 12-hour fasting period and the animals were euthanized and livers collected 4 hours later, after 4 hour exposure to food (28 hours after the final RA dose). To determine

Molecular Pharmacology Fast Forward. Published on February 26, 2016 as DOI: 10.1124/mol.116.103697
This article has not been copyedited and formatted. The final version may differ from this version.

whether inhibition of CYP26 enzymes has similar effects as *at*RA administration on mouse liver, adult (~90 dpp) male mice were treated twice daily (every 12 hours) for three consecutive days with 2.5 mg/kg talarozole (Active Biochem, Maplewood NJ, USA) dissolved in polyethylene glycol (PEG) 300 or vehicle control. Twelve hours after the final dose the animals were euthanized and livers collected. mRNA was extracted from 50-100 mg liver tissue and qRT-PCR used to determine changes in target mRNA as described above. β-Actin was used as the housekeeping gene. To quantify mitochondrial number, SDHA expression was determined by western blotting as described above and mitochondria number was quantified from genomic DNA using qPCR as described above.

Statistical Analysis. Statistical analyses were conducted using GraphPad prism v.5 statistical software. All differences involving multiple comparisons were tested using one-way ANOVA with Tukey test as the post hoc analysis, while single comparisons were done using Student's t-test. Data are expressed as mean ± SD; $p<0.05$ was considered significant.

Results

Proteomic analysis of *at*RA signaling in the liver: *at*RA treatment had no effect on HepG2 cell proliferation or viability at *at*RA concentrations from 0.001 to 50 μM over the 72 hour treatment (Figure 1A), confirming that alterations in protein or mRNA expression were not due to altered number of cells. Based on the proteomic analysis of HepG2 cells treated with 10 μM *at*RA for 72 hours, the expression of 59 proteins in several functional categories was significantly altered by *at*RA treatment (Table 1). This was a small fraction (<0.1%) of all proteins detected in the experiment. Table 1 lists those proteins for which the same peptides were detected reliably in all analyzed samples. Almost half of the proteins (24 of 59, 41%) whose

Molecular Pharmacology Fast Forward. Published on February 26, 2016 as DOI: 10.1124/mol.116.103697
This article has not been copyedited and formatted. The final version may differ from this version.

expression was significantly altered were proteins involved in lipid metabolism (Figure 1B) suggesting that one of the major effects of *at*RA in the liver is modulating fatty acid oxidation and lipid metabolism. Based on the proteomic analysis, *at*RA treatment significantly increased expression of enzymes involved in fatty acid β-oxidation such as ACSL3, ACSL4, ACAD and ECH1, isocitrate dehydrogenase (IDH2), a key enzyme involved in TCA cycle and ATP synthase (ATP5A1), the mitochondrial respiratory chain complex V (Figure 1B). In agreement with proteomic findings, the mRNA levels of CPT1α, the rate limiting enzyme for fatty acid oxidation and ATGL, a triglyceride specific lipase involved in triglyceride hydrolysis was significantly increased (Figure 1C) in HepG2 cells at 1 and 10 μM *at*RA treatment. Interestingly, *at*RA treatment at 1 μM had no effect on mRNA levels of SREBP1c and DGAT2, which are involved in fatty acid and triglyceride synthesis, nor did *at*RA treatment alter the mRNA levels of MTTP, an enzyme involved in VLDL synthesis and secretion (Figure 1C). However, at 10 μM, *at*RA increased SREBP1c mRNA (a key transcription factor for *de novo* fatty acid synthesis) (Figure 1C) and FASN protein, which is regulated by SREBP1 (Figure 1B). Taken together the proteomics and mRNA analysis suggest that *at*RA increases mitochondrial fatty acid oxidation in the HepG2 cells at physiologically relevant concentrations, and may increase fatty acid synthesis at supra-physiological concentrations.

Effects of *at*RA on mitochondrial biogenesis markers in models of healthy human liver: Based on the proteomic data, that suggested that mitochondrial fatty acid oxidation was increased, the mRNA expression of key mitochondrial biogenesis markers PGC1α, PGC1β and NRF1 were measured in HepG2 cells treated with 1 μM *at*RA for 24 hours. The mRNA of PGC1α, PGC1β and NRF1 was increased 2-3 fold ($p<0.05$) in the HepG2 cells suggesting increased mitochondrial biogenesis in response to *at*RA treatment (Figure 2A). In agreement

Molecular Pharmacology Fast Forward. Published on February 26, 2016 as DOI: 10.1124/mol.116.103697
This article has not been copyedited and formatted. The final version may differ from this version.

with the mRNA data, ATP production was significantly increased following treatment with 1 μM *at*RA (Figure 2B) suggesting mitochondrial function was also increased.

Considerable depletion of *at*RA was observed in the treated cells at 24 hours of treatment with 1 μM *at*RA. *at*RA concentrations decreased by 87% to 129 ± 19.15 nM after 24 hours (Table 2). To test whether inhibition of CYP26 (the main enzyme metabolizing *at*RA) increases *at*RA concentrations and potency, HepG2 cells were treated with *at*RA together with talarozole, a CYP26 inhibitor, and *at*RA concentrations and mitochondrial biogenesis markers and ATP production were measured. In the presence of talarozole *at*RA concentrations were 2.6-fold higher at the end of the 24-hour treatment than when cells were treated with *at*RA alone while the concentrations of the metabolites of *at*RA were decreased upon talarozole treatment (Table 2). The increased exposure of the cells to *at*RA was reflected in 2-3 fold higher PGC1α, PGC1β and NRF1 mRNA induction in the presence of talarozole together with *at*RA when compared to *at*RA alone (Figure 2A). Talarozole treatment with *at*RA also resulted in approximately 2-fold greater ATP production in HepG2 cells when compared to *at*RA treatment alone (Figure 2B). Surprisingly, talarozole alone also increased ATP production, PGC1β and NRF1 mRNA expression but not PGC1α mRNA.

To confirm that the observed changes in the mRNA of mitochondrial biogenesis genes after *at*RA treatment result in improved mitochondrial function and increased mitochondrial number and fatty acid oxidation, the protein expression of SDHA, a marker for increase in mitochondrial content was measured together with mitochondrial DNA and fatty acid β-oxidation. In HepG2 cells 1 μM *at*RA treatment increased SDHA protein expression 2-fold (Figure 2C and 2D) and 1-10 μM *at*RA treatment increased fatty acid β-oxidation 2-3 fold,

Molecular Pharmacology Fast Forward. Published on February 26, 2016 as DOI: 10.1124/mol.116.103697
This article has not been copyedited and formatted. The final version may differ from this version.

compared to vehicle treated cells (Figure 2E). Mitochondrial DNA was increased 4 to 5-fold following *at*RA treatment (Figure 2F).

To further translate the findings from HepG2 cells to human liver, the effect of *at*RA on mitochondrial function and biogenesis was evaluated in human hepatocytes from three donors. Similar to the HepG2 cells, in human hepatocytes the mRNA expression of PGC1α, PGC1β and NRF1 was increased 2-5 fold ($p<0.05$), compared to vehicle treated group (Figure 3A). In addition, *at*RA increased ATP production by 2-3 fold compared to vehicle treated human hepatocytes. *at*RA treatment also increased SDHA protein expression 2-3 fold (Figure 3C) and mitochondrial DNA 2-7 fold (Figure 3D) demonstrating that *at*RA increases mitochondria number and function in human hepatocytes.

To explore the potential nuclear receptors responsible for the effects of *at*RA on mitochondrial biogenesis, the effect of *at*RA on the mRNA expression of RARs and PPARs was tested. *at*RA significantly increased the mRNA expression of RARβ and PPARδ, but had no effect on RARα, PPARα or PPARγ (Supplementary Figure 1A). This suggests that the effect of *at*RA on mitochondrial biogenesis may be a combination of RARβ and PPARδ activation. The role of RARβ and PPARδ in the induction of the genes and processes of interest was further studied using selective RAR and PPAR agonists in comparison to *at*RA. While the PPARδ agonist GW0742 induced PGC1β and NRF1, PGC1α was not changed. In contrast the RAR pan agonist TTNPB had no effect on PGC1α, PGC1β and NRF1 mRNA expression alone or in combination with *at*RA (Supplemental Figure 1B). Interestingly, when GW0742 was used together with *at*RA, the mRNA induction of PGC1β and NRF1 was greater than with *at*RA alone while the induction of PGC1α was similar. Together these results suggested that RARs are not involved in the induction of mitochondrial biogenesis or function.

Molecular Pharmacology Fast Forward. Published on February 26, 2016 as DOI: 10.1124/mol.116.103697
This article has not been copyedited and formatted. The final version may differ from this version.

To further explore the role of specific nuclear receptors in the increase in mitochondrial biogenesis markers by *at*RA, RARα, RARβ and PPARδ siRNAs were used. The RARα, RARβ and PPARδ siRNA decreased the corresponding nuclear receptor mRNA levels by 75%, 80% and 60%, respectively (Supplemental Figure 2A). The RARβ and PPARδ siRNA also decreased RARβ and PPARδ protein expression respectively by 50-60% in *at*RA treated cells when compared to *at*RA plus scrambled siRNA treated controls (Supplemental Figure 2B-D). In contrast, RARβ siRNA had no effect on the induction of PPARδ by *at*RA and PPARδ siRNA had no effect on the induction of RARβ by *at*RA (Supplemental Figure 2B-D). RARα and RARβ siRNA had no effect on the induction of PGC1α, PGC1β and NRF1 mRNA by *at*RA (Figure 4A). In contrast, PPARδ siRNA significantly decreased the induction of PGC1α, PGC1β and NRF1 mRNA by *at*RA when compared to scrambled siRNA control (Figure 4A), suggesting that these effects of *at*RA in the HepG2 cells are mediated by PPARδ. In agreement with the role of PPARδ in the regulation of mitochondrial function and biogenesis, PPARδ siRNA eliminated the increase in ATP production by *at*RA as well as the induction of SDHA protein expression and increase in β-oxidation (Figure 4 B-E). PPARδ siRNA also significantly deceased the *at*RA mediated induction of mitochondrial DNA (Figure 4F).

Effects of *at*RA on mitochondrial biogenesis markers in models of human fatty liver: Lipid loaded HepG2 cells and primary human hepatocytes were used as a model of human fatty liver. Lipid accumulation was confirmed via Oil Red O staining (Figure 5A). In lipid loaded HepG2 cells PGC1α, PGC1β and NRF1 mRNA was increased 2-3 fold ($p<0.05$) in response to *at*RA treatment (Figure 5B), a finding in excellent agreement with the normal HepG2 cells. In lipid loaded HepG2 cells 1 μM *at*RA treatment resulted in a dose dependent increase in ATP production (Figure 5C). Similarly in lipid loaded HepG2 cells *at*RA treatment also increased

Molecular Pharmacology Fast Forward. Published on February 26, 2016 as DOI: 10.1124/mol.116.103697
This article has not been copyedited and formatted. The final version may differ from this version.

SDHA protein expression 2-fold (Figure 5D). The effect of talarozole on the potency of *at*RA as an inducer of mitochondrial biogenesis genes and ATP production was also similar in lipid loaded HepG2 cells (Figure 5B and C) as in normal HepG2 cells. The induction of PGC1α, PGC1β and NRF1 mRNA and ATP production was significantly greater when lipid loaded HepG2 cells were co-treated with talarozole and *at*RA than with *at*RA alone at 100 nM (Figure 5B and C). In excellent agreement with the lipid loaded HepG2 cell data and normal human hepatocyte experiments, in lipid loaded human hepatocytes from 3 donors the mRNA expression of PGC1α, PGC1β and NRF1 was increased 2-4 fold ($p<0.05$) and ATP production was increased 2-3 fold, compared to vehicle treated group in each of the three donors (Figure 5 E-F).

Similar to normal HepG2 cells, *at*RA significantly increased the transcription of both RARβ and PPARδ in lipid loaded HepG2 cells (Figure 6A). Interestingly, in lipid loaded HepG2 cells RARα was also induced by *at*RA treatment. When siRNA for each of the nuclear receptors was used in the lipid loaded HepG2 cells, only PPARδ knock down attenuated the *at*RA mediated induction of PGC1α, PGC1β and NRF1 mRNA (Figure 6B-D). RARβ and RARα knock down had no effect on the induction of PGC1α, PGC1β and NRF1 mRNA by *at*RA in the lipid loaded cells.

Effect of increased *at*RA concentrations on the expression of mitochondrial biogenesis in vivo in mouse liver: To evaluate whether the in vitro findings of the effects of *at*RA on hepatic mitochondrial biogenesis in human liver models translate to in vivo, mice were treated with vehicle or *at*RA for 5 days and hepatic mRNA expression of Pgc1α, Pgc1β, Nrf1, Cpt1α, and Atgl was measured following an overnight fast or after feeding (Figure 7). *at*RA treatment resulted in up to 6-fold ($p<0.05$) increase in the mRNA of Pgc1α, Pgc1β, Nrf1 and Cpt1α (Figure 7A) but had no effect on Atgl expression in fasted condition. The induction of

Molecular Pharmacology Fast Forward. Published on February 26, 2016 as DOI: 10.1124/mol.116.103697
This article has not been copyedited and formatted. The final version may differ from this version.

Pgc1α, Pgc1β, Nrf1 and Cpt1α was accompanied with increased mitochondrial DNA and SDHA expression in the mouse liver following *at*RA treatment in fasted condition (Figure 7B-D). However, 4 hours later, after refeeding of the mice, *at*RA no longer affected any of the above mentioned markers (Figure 7A-D). The induction of the marker genes of RAR activation, Cyp26a1 and Rarβ, was much more modest than the induction of mitochondrial biogenesis marker genes. Rarβ, was induced approximately 2.5-fold ($p<0.05$) but there was no significant increase in Cyp26a1 mRNA (1.7-fold, $p>0.05$) following *at*RA treatment (Figure 7E). Unlike mitochondrial biogenesis markers, there was no difference in Rarβ induction between fed and fasted groups (Figure 7), a finding in agreement with different induction mechanisms and mRNA half-lives for these target genes.

To increase the exposure of endogenous *at*RA in the liver, male C57BL/6X129 mice were treated with talarozole, an inhibitor of Cyp26, and mRNA expression of key mitochondrial biogenesis genes was measured. Similar to *at*RA treatment, talarozole treatment increased mRNA expression of Pgc1β and Nrf1 5-10 fold ($p<0.05$) but the 4-fold increase in Pgc1α mRNA was not significant ($p>0.05$) (Figure 7F).

Discussion

Treatment of most cancer cell lines in vitro, or neuroblastoma and acute promyelocytic leukemia in vivo with RA leads to apoptosis and cell cycle arrest manifesting the classic RAR mediated effects of *at*RA regulating cell proliferation. Interestingly, in models of human liver, treatment with *at*RA had no effect of cell viability or proliferation at concentrations that typically lead to cell cycle arrest and apoptosis. This result led us to evaluate *at*RA signaling in HepG2 cells using a proteomic approach. The proteomic studies showed that instead of cell cycle

Molecular Pharmacology Fast Forward. Published on February 26, 2016 as DOI: 10.1124/mol.116.103697
This article has not been copyedited and formatted. The final version may differ from this version.

regulation, *at*RA treatment predominantly altered the expression of proteins responsible for regulating lipid and fatty acid metabolism in the human liver models. These findings led to the identification of a novel effect of *at*RA signaling in the liver. The indication of the proteomic study that *at*RA alters lipid and fatty acid metabolism was intriguing as use of retinoids and RA isomers isotretinoin (13-*cis*RA) and alitretinoin (9-*cis*RA) in dermatology and in cancer treatment is associated with changes in lipid and lipoprotein metabolism including hypertriglyceridemia, hypercholesterolemia, increased total cholesterol and decreased HDL-cholesterol in about third of the treated patients (Brelsford and Beute, 2008; Lawrence et al., 2001; Lilley et al., 2013; Staels, 2001). The induction of SREBP1 mRNA observed in this study following treatment with 10 μM *at*RA is in agreement with the clinical findings as the 10 μM *at*RA treatment closely mimics the RA exposures observed following retinoid therapy. The 1 μM treatments used in the subsequent experiments in this study are expected to closely mimic endogenous *at*RA concentrations in the liver as the measured media concentrations during treatment were approximately 100 nM. The low media concentrations measured are likely due to extensive metabolism of *at*RA in the cells as reported previously (Topletz et al., 2015) and partitioning and nonspecific binding of *at*RA into cells. Strikingly, at the concentrations of *at*RA (100 nM and 1 μM) that reflect changes in endogenous *at*RA concentrations, SREBP1 mRNA was not increased despite consistent changes in other proteins and mRNA. This suggests that at different concentrations of *at*RA different nuclear receptors and signaling pathways are activated, leading to different effects on lipid metabolism.

In addition to SREBP1 induction, the proteomic study identified an increase in a complement of proteins that contribute to fatty acid oxidation, mitochondrial function and mitochondrial energy production leading to a hypothesis that *at*RA increases mitochondrial

Molecular Pharmacology Fast Forward. Published on February 26, 2016 as DOI: 10.1124/mol.116.103697
This article has not been copyedited and formatted. The final version may differ from this version.

biogenesis and fatty acid β-oxidation in the liver. The subsequent mechanistic studies shown here consistently support a beneficial, regulatory role of endogenous *at*RA on lipid homeostasis. The studies show that *at*RA increases mitochondrial number (mitochondrial DNA and SDHA expression), mitochondrial function (ATP production) and fatty acid β-oxidation (^{14}C palmitate oxidation) in normal and fatty human liver. The collective pathways and proteins affected by *at*RA treatment are summarized in Figure 8. It should, however, be noted that the increase observed in palmitate oxidation may also be partially due to increased peroxisomal fatty acid oxidation and further studies are needed to characterize the complete effects of *at*RA on liver lipid homeostasis.

Previous mouse studies have suggested that *at*RA increases fatty acid oxidation and decreases hepatic lipid accumulation predominantly via RAR mediated processes. *at*RA has been shown to suppress PPARγ2 expression and decrease hepatic lipid accumulation in diet induced obese mice by activating RARα (Kim et al., 2014). After adenoviral overexpression of RARβ, *at*RA treatment increased the expression of fatty acid oxidative genes CPT1α and MCAD in mouse liver and in HepG2 cells (Li et al., 2013). *at*RA also enhanced fatty acid oxidation and ketogenesis via RAR activation and FGF21 induction in HepG2 cells (Amengual et al., 2012; Li et al., 2013). While the data presented in this study in human hepatocytes, HepG2 cells and in mice is in agreement with a role of *at*RA at endogenous concentrations in increasing fatty acid β-oxidation, ATP production, mitochondrial function, the mRNA levels of mitochondrial biogenesis markers and mitochondria number, the data does not support a role of RARs in how *at*RA regulates these processes. While *at*RA clearly activates RARs in the HepG2 cells based on the observed induction of RARβ mRNA, the siRNA studies and chemical agonist experiments show that the regulation of mitochondrial function by *at*RA is likely mediated by PPARδ, as

Molecular Pharmacology Fast Forward. Published on February 26, 2016 as DOI: 10.1124/mol.116.103697
This article has not been copyedited and formatted. The final version may differ from this version.

only PPARδ siRNA decreased the *at*RA mediated induction of mitochondrial biogenesis genes, mitochondrial DNA content, ATP production and fatty acid oxidation. Importantly, PPARδ silencing had similar, consistent, effects on all markers of mitochondrial biogenesis and fatty acid β-oxidation suggesting that *at*RA mediates all of these processes via similar mechanism. The proposed mechanism via PPARδ is shown in Figure 8. The in vivo studies in mice are in agreement with this interpretation of predominant role of PPARδ, as *at*RA treatment resulted in only modest effects on the mRNA levels of RAR target genes CYP26A1 and RARβ, but had significant effects on the expression of mitochondrial biogenesis genes which are believed to be PPARδ targets. Yet, it is possible that the modest effects on CYP26A1 and RARβ mRNA in mice are due to the short mRNA half-life of these genes and *at*RA as the induction was analyzed 24-28 hours after last *at*RA dose. The findings of the role of PPARδ in RA signaling are in agreement with previous studies that documented that cellular retinoic acid binding protein II (CRABPII) and fatty acid binding protein-5 (FABP5) direct *at*RA to the nuclear receptors RAR and PPARβ/δ, respectively, and that the pleotropic effects of *at*RA are due to activation of both of these receptors (Berry and Noy, 2012; Bonet et al., 2012; Napoli, 1996; Obrochta et al., 2015; Schug et al., 2007). However, we also show that *at*RA treatment increases PPARβ/δ mRNA, and it is possible that this induction in part or solely contributes to the observed effects on mitochondrial biogenesis without *at*RA binding directly to PPARβ/δ.

Altered vitamin A homeostasis is well documented in alcoholic liver disease but recent reports associate altered vitamin A homeostasis also with NAFLD and steatosis (Ashla et al., 2010; Kim et al., 2014; Liu et al., 2015; Trasino et al., 2015). For example, human liver biopsies of NAFLD and non-alcoholic steatohepatitis (NASH) patients demonstrated increased expression of the main enzyme metabolizing *at*RA, CYP26A1, suggesting that *at*RA is depleted

Molecular Pharmacology Fast Forward. Published on February 26, 2016 as DOI: 10.1124/mol.116.103697
This article has not been copyedited and formatted. The final version may differ from this version.

in livers of these patients (Ashla et al., 2010). This is likely deleterious in NAFLD as we show that *at*RA increases mitochondrial biogenesis and fatty acid oxidation in models of fatty liver and NAFLD. As NAFLD is associated with decreased mitochondrial function (Aharoni-Simon et al., 2011; Handa et al., 2014; Sookoian et al., 2010), this data suggests that decreasing *at*RA concentrations in NAFLD may contribute to decreasing mitochondrial function and disease progression, and that increasing *at*RA concentrations in NAFLD may be beneficial and result in improvement of mitochondrial function and fatty acid oxidation. Such increases in endogenous *at*RA concentrations could be achieved for example via inhibition of the CYP26 enzymes as shown here with talarozole treatment in HepG2 cells and in mice. In the HepG2 cells talarozole decreased *at*RA metabolism increasing *at*RA concentrations and thus potentiating the effects of *at*RA on mitochondrial biogenesis. Similarly, in vivo in mice, talarozole treatment increased the expression of mitochondrial biogenesis genes suggesting that increasing endogenous *at*RA concentrations in the liver is sufficient to obtain the effects observed in HepG2 cells and human hepatocytes following *at*RA treatment. Consistent with the human liver models, *at*RA treatment increased the expression of PGC1α, PGC1β, NRF1 and CPT1α under fasting conditions in mice and increased mitochondrial number and SDHA protein. As expected from the energy needs of fed mice, after refeeding the mice had low expression of PGC1α, PGC1β, NRF1, ATGL and CPT1α compared to fasted mice and *at*RA did not have equivalent effects on mitochondrial number and function after feeding as in the fasted mice. Yet, it is also possible that due to the longer time interval between last *at*RA dose and collection of samples in the fed mice when compared to fasted, the effects of *at*RA were no longer observed in the fed mice. Further studies are needed to fully explore the differences in *at*RA signaling under fasted and fed conditions.

.

Molecular Pharmacology Fast Forward. Published on February 26, 2016 as DOI: 10.1124/mol.116.103697
This article has not been copyedited and formatted. The final version may differ from this version.

In summary, this study shows that *at*RA increases mitochondrial biogenesis, fatty acid β-oxidation, expression of mitochondrial respiratory chain components and ATP production in models of healthy and fatty human liver and in vivo in mouse liver and these effects are predominantly regulated through PPARδ signaling instead of RAR activation. Moreover, increasing *at*RA concentration by CYP26 inhibition potentiated *at*RA effects on mitochondrial biogenesis and ATP production in cell models and in vivo in mice. Taken together the increased expression of CYP26A1 in NAFLD and the observed efficacy of a CYP26 inhibitor in mice and in human liver models suggests that CYP26 inhibition would be beneficial in NAFLD and result in increased mitochondrial fatty acid oxidation and mitochondrial biogenesis.

Acknowledgements

The authors wish to thank Dr. Alan Chait of NORC, University of Washington for his advice on the fatty acid oxidation assay and Faith Stevison, MS for her skillful assistance with LC-MS/MS.

Authorship Contributions

Participated in research design: Tripathy, Chapman, Hogarth, Isoherranen

Conducted experiments: Tripathy, Chapman, Han, Hogarth, Arnold, Oken, Kent

Contributed new reagents or analytical tools: Chapman, Goodlett

Wrote or contributed to the writing of the manuscript: Tripathy, Chapman, Han, Hogarth, Isoherranen

Molecular Pharmacology Fast Forward. Published on February 26, 2016 as DOI: 10.1124/mol.116.103697
This article has not been copyedited and formatted. The final version may differ from this version.

References

Aharoni-Simon M, Hann-Obercyger M, Pen S, Madar Z, and Tirosh O (2011) Fatty liver is associated with impaired activity of PPARgamma-coactivator 1alpha (PGC1alpha) and mitochondrial biogenesis in mice. *Lab Invest* **91**: 1018-1028.

Amengual J, Petrov P, Bonet ML, Ribot J, and Palou A (2012) Induction of carnitine palmitoyl transferase 1 and fatty acid oxidation by retinoic acid in HepG2 cells. *Int J Biochem Cell Biol* **44**: 2019-2027.

Ashla AA, Hoshikawa Y, Tsuchiya H, Hashiguchi K, Enjoji M, Nakamuta M, Taketomi A, Maehara Y, Shomori K, Kurimasa A, Hisatome I, Ito H, and Shiota G (2010) Genetic analysis of expression profile involved in retinoid metabolism in non-alcoholic fatty liver disease. *Hepatol Res* **40**: 594-604.

Bell H, Nilsson A, Norum KR, Pedersen LB, Raknerud N, and Rasmussen M (1989) Retinol and retinyl esters in patients with alcoholic liver disease. *J Hepatol* **8**: 26-31.

Berry DC, and Noy N (2007) Is PPARbeta/delta a Retinoid Receptor? *PPAR Res* 2007: 73256.

Berry DC, and Noy N (2009) All-trans-retinoic acid represses obesity and insulin resistance by activating both peroxisome proliferation-activated receptor beta/delta and retinoic acid receptor. *Mol Cell Biol* **29**: 3286-3296.

Berry DC, and Noy N (2012) Signaling by vitamin A and retinol-binding protein in regulation of insulin responses and lipid homeostasis. *Biochim Biophys Acta* **1821**: 168-176.

Bershad S, Rubinstein A, Paterniti JR, Le NA, Poliak SC, Heller B, Ginsberg HN, Fleischmajer R, and Brown WV (1985) Changes in plasma lipids and lipoproteins during isotretinoin therapy for acne. *N Engl J Med* **313**: 981-985.

Betancourt AM, King AL, Fetterman JL, Millender-Swain T, Finley RD, Oliva CR, Crowe DR, Ballinger SW, and Bailey SM (2014) Mitochondrial-nuclear genome interactions in non-alcoholic fatty liver disease in mice. *Biochem J* **461**: 223-232.

Bonet ML, Ribot J, and Palou A (2012) Lipid metabolism in mammalian tissues and its control by retinoic acid. *Biochim Biophys Acta* **1821**: 177-189.

Brelsford M, and Beute TC (2008) Preventing and managing the side effects of isotretinoin. *Semin Cutan Med Surg* **27**: 197-206.

Chapman JD, Edgarl JS, Goodlett DR, and Goo YA (2015) Use of captive spray ionization to increase throughput of the data-independent acquisition technique PAcIFIC. *Rapid Commun Mass Spectrom*.

Clugston RD, Jiang H, Lee MX, Berk PD, Goldberg IJ, Huang LS, and Blaner WS (2013) Altered hepatic retinyl ester concentration and acyl composition in response to alcohol consumption. *Biochim Biophys Acta* **1831**: 1276-1286.

Handa P, Maliken BD, Nelson JE, Morgan-Stevenson V, Messner DJ, Dhillon BK, Klintworth HM, Beauchamp M, Yeh MM, Elfers CT, Roth CL, and Kowdley KV (2014) Reduced adiponectin signaling due to weight gain results in nonalcoholic steatohepatitis through impaired mitochondrial biogenesis. *Hepatology* **60**: 133-145.

Havilio M, Haddad Y, and Smilansky Z (2003) Intensity-based statistical scorer for tandem mass spectrometry. *Anal Chem* **75**: 435-444.

Keller A, Nesvizhskii AI, Kolker E, and Aebersold R (2002) Empirical statistical model to estimate the accuracy of peptide identifications made by MS/MS and database search. *Anal Chem* **74**: 5383-5392.

Kim SC, Kim CK, Axe D, Cook A, Lee M, Li T, Smallwood N, Chiang JY, Hardwick JP, Moore DD, and Lee YK (2014) All-trans-retinoic acid ameliorates hepatic steatosis in mice by a novel transcriptional cascade. *Hepatology* **59**: 1750-1760.

Koh KH, Pan X, Shen HW, Arnold SL, Yu AM, Gonzalez FJ, Isoherranen N, and Jeong H (2014) Altered expression of small heterodimer partner governs cytochrome P450 (CYP) 2D6 induction during pregnancy in CYP2D6-humanized mice. *J Biol Chem* **289**: 3105-3113.

Lawrence JA, Adamson PC, Caruso R, Chow C, Kleiner D, Murphy RF, Venzon DJ, Shovlin M, Noone M, Merino M, Cowan KH, Kaiser M, O'Shaughnessy J, and Zujewski J (2001) Phase I clinical trial of alitretinoin and tamoxifen in breast cancer patients: toxicity, pharmacokinetic, and biomarker evaluations. *J Clin Oncol* **19**: 2754-2763.

Lee YS, and Jeong WI (2012) Retinoic acids and hepatic stellate cells in liver disease. *J Gastroenterol Hepatol* **27** Suppl 2: 75-79.

Li Y, Wong K, Walsh K, Gao B, and Zang M (2013) Retinoic acid receptor beta stimulates hepatic induction of fibroblast growth factor 21 to promote fatty acid oxidation and control whole-body energy homeostasis in mice. *J Biol Chem* **288**: 10490-10504.

Lilley JS, Linton MF, and Fazio S (2013) Oral retinoids and plasma lipids. *Dermatol Ther* **26**: 404-410.

Liu H, Sadygov RG, and Yates JR, 3rd (2004) A model for random sampling and estimation of relative protein abundance in shotgun proteomics. *Anal Chem* **76**: 4193-4201.

Liu Y, Chen H, Wang J, Zhou W, Sun R, and Xia M (2015) Association of serum retinoic acid with hepatic steatosis and liver injury in nonalcoholic fatty liver disease. *Am J Clin Nutr* **102**: 130-137.

Mamoon A, Subauste A, Subauste MC, and Subauste J (2014) Retinoic acid regulates several genes in bile acid and lipid metabolism via upregulation of small heterodimer partner in hepatocytes. *Gene* **550**: 165-170.

McClintick JN, Crabb DW, Tian H, Pinaire J, Smith JR, Jerome RE, and Edenberg HJ (2006) Global effects of vitamin A deficiency on gene expression in rat liver: evidence for hypoandrogenism. *J Nutr Biochem* **17**: 345-355.

Moriwaki H, Blaner WS, Piantedosi R, and Goodman DS (1988) Effects of dietary retinoid and triglyceride on the lipid composition of rat liver stellate cells and stellate cell lipid droplets. *J Lipid Res* **29**: 1523-1534.

Napoli JL (1996) Biochemical pathways of retinoid transport, metabolism, and signal transduction. *Clin Immunol Immunopathol* **80**: S52-62.

Nesvizhskii AI, Keller A, Kolker E, and Aebersold R (2003) A statistical model for identifying proteins by tandem mass spectrometry. *Anal Chem* **75**: 4646-4658.

O'Byrne SM, and Blaner WS (2013) Retinol and retinyl esters: biochemistry and physiology. *J Lipid Res* **54**: 1731-1743.

Obrochta KM, Krois CR, Campos B, and Napoli JL (2015) Insulin Regulates Retinol Dehydrogenase Expression and all-trans-Retinoic Acid Biosynthesis through FoxO1. *J Biol Chem* **290**: 7259-68.

Oliveros LB, Domeniconi MA, Vega VA, Gatica LV, Brigada AM, and Gimenez MS (2007) Vitamin A deficiency modifies lipid metabolism in rat liver. *Br J Nutr* **97**: 263-272.

Paik J, Haenisch M, Muller CH, Goldstein AS, Arnold S, Isoherranen N, Brabb T, Treuting PM, and Amory JK (2014) Inhibition of retinoic acid biosynthesis by the

bisdichloroacetyldiamine WIN 18,446 markedly suppresses spermatogenesis and alters retinoid metabolism in mice. *J Biol Chem* **289**: 15104-15117.

Panchaud A, Jung S, Shaffer SA, Aitchison JD, and Goodlett DR (2011) Faster, quantitative, and accurate precursor acquisition independent from ion count. *Anal Chem* **83**: 2250-2257.

Panchaud A, Scherl A, Shaffer SA, von Haller PD, Kulasekara HD, Miller SI, and Goodlett DR (2009) Precursor acquisition independent from ion count: how to dive deeper into the proteomics ocean. *Anal Chem* **81**: 6481-6488.

Pessayre D (2007) Role of mitochondria in non-alcoholic fatty liver disease. *J Gastroenterol Hepatol* **22** Suppl 1: S20-27.

Ryu S, Gallis B, Goo YA, Shaffer SA, Radulovic D, and Goodlett DR (2008) Comparison of a label-free quantitative proteomic method based on peptide ion current area to the isotope coded affinity tag method. *Cancer Inform* **6**: 243-255.

Schug TT, Berry DC, Shaw NS, Travis SN, and Noy N (2007) Opposing effects of retinoic acid on cell growth result from alternate activation of two different nuclear receptors. *Cell* **129**: 723-733.

Shaw N, Elholm M, and Noy N (2003) Retinoic acid is a high affinity selective ligand for the peroxisome proliferator-activated receptor beta/delta. *J Biol Chem* **278**: 41589-41592.

Sookoian S, Rosselli MS, Gemma C, Burgueno AL, Fernandez Gianotti T, Castano GO, and Pirola CJ (2010) Epigenetic regulation of insulin resistance in nonalcoholic fatty liver disease: impact of liver methylation of the peroxisome proliferator-activated receptor gamma coactivator 1alpha promoter. *Hepatology* **52**: 1992-2000.

Staels B (2001) Regulation of lipid and lipoprotein metabolism by retinoids. *J Am Acad Dermatol* **45**: S158-167.

Tay S, Dickmann L, Dixit V, and Isoherranen N (2010) A comparison of the roles of peroxisome proliferator-activated receptor and retinoic acid receptor on CYP26 regulation. *Mol Pharmacol* **77**: 218-227.

Topletz AR, Tripathy S, Foti RS, Shimshoni JA, Nelson WL, and Isoherranen N (2015) Induction of CYP26A1 by metabolites of retinoic acid: evidence that CYP26A1 is an important enzyme in the elimination of active retinoids. *Mol Pharmacol* **87**: 430-441.

Trasino SE, Tang XH, Jessurun J, and Gudas LJ (2015) Obesity Leads to Tissue, but not Serum Vitamin A Deficiency. *Sci Rep* 5: 15893.

Ward RJ, and Peters TJ (1992) The antioxidant status of patients with either alcohol-induced liver damage or myopathy. *Alcohol Alcohol* **27**: 359-365.

Wei Y, Rector RS, Thyfault JP, and Ibdah JA (2008) Nonalcoholic fatty liver disease and mitochondrial dysfunction. *World J Gastroenterol* **14**: 193-199.

Wolf G (2010) Retinoic acid activation of peroxisome proliferation-activated receptor delta represses obesity and insulin resistance. *Nutr Rev* **68**: 67-70.

Yanagitani A, Yamada S, Yasui S, Shimomura T, Murai R, Murawaki Y, Hashiguchi K, Kanbe T, Saeki T, Ichiba M, Tanabe Y, Yoshida Y, Morino S, Kurimasa A, Usuda N, Yamazaki H, Kunisada T, Ito H, and Shiota G (2004) Retinoic acid receptor alpha dominant negative form causes steatohepatitis and liver tumors in transgenic mice. *Hepatology* **40**: 366-375.

Yang F, He Y, Liu HX, Tsuei J, Jiang X, Yang L, Wang ZT, and Wan YJ (2014) All-trans retinoic acid regulates hepatic bile acid homeostasis. *Biochem Pharmacol* **91**: 483-489.

Yu S, Levi L, Siegel R, and Noy N (2012) Retinoic acid induces neurogenesis by activating both retinoic acid receptors (RARs) and peroxisome proliferator-activated receptor beta/delta (PPARbeta/delta). *J Biol Chem* **287**: 42195-42205.

Molecular Pharmacology Fast Forward. Published on February 26, 2016 as DOI: 10.1124/mol.116.103697
This article has not been copyedited and formatted. The final version may differ from this version.

Footnotes

This research was supported by grants from National Institutes of health [Grants R01 GM111772, R01 GM081569, R01 GM081569-S1 and P30 DK035816].

Molecular Pharmacology Fast Forward. Published on February 26, 2016 as DOI: 10.1124/mol.116.103697
This article has not been copyedited and formatted. The final version may differ from this version.

Legends for Figures

Figure 1. *at*RA increases the protein and mRNA expression of enzymes involved in fatty acid oxidation in HepG2 cells. (A) Cell viability following treatment of HepG2 cells with increasing concentrations of *at*RA. Cell proliferation is shown as mean ± SD, n = 6. (B) Heat map for the effects of 10 μM *at*RA treatment in comparison to vehicle (DMSO) on expression of enzymes involved in different metabolic pathways as determine by the proteomic analysis. (C) The effect of *at*RA treatment (1 and 10 μM) on the mRNA expression of enzymes involved in lipid metabolism. mRNA results are expressed as mean ± SD, n = 3 and are representative of at least 3 separate studies. ***** indicates $p<0.05$ in comparison to vehicle treated controls Student's t-test.

Figure 2. *at*RA increases mitochondrial biogenesis, ATP production and fatty acid β-oxidation in normal HepG2 cells. (A) The effect of *at*RA (1 μM) and talarozole co-treatment on mRNA expression of mitochondrial biogenesis genes. (B) The effects of *at*RA and talarozole co-treatment on ATP production. (C and D) Induction of SDHA protein following treatment with *at*RA as measured by western blotting. Panel C shows the quantification of the representative western blot shown in panel D. The blot shows analysis of three independent biological replicates. (E) The effects of *at*RA treatment on palmitate oxidation as a measure of increased β-oxidation. (F) The effect of *at*RA treatment on mitochondrial DNA copy number. All experiments were conducted as described in the experimental section. Results are expressed as mean ± SD, n = 3. Comparisons between vehicle (ethanol) and *at*RA treated cells were made by Student's t-test: ***** indicates $p<0.05$ in comparison to vehicle treated controls. # indicates $p<0.05$ in comparison to 1 μM *at*RA treated controls.

Molecular Pharmacology Fast Forward. Published on February 26, 2016 as DOI: 10.1124/mol.116.103697
This article has not been copyedited and formatted. The final version may differ from this version.

Figure 3. *at*RA increases mitochondrial biogenesis and ATP production in normal human hepatocytes. (A) Induction of the mRNA expression of key mitochondrial biogenesis genes (PGC1α, PGC1β and NRF1) by 1 μM *at*RA. All data is shown as fold increase in comparison to vehicle control. (B) Induction of ATP production by 1 μM *at*RA in three independent human hepatocyte donors. (C) Induction of SDHA protein in three individual human hepatocyte donors following treatment with 1 μM *at*RA as measured by western blotting. The quantification of the replicate western blots and a representative blot of duplicate treatments in three donors is shown. (D) The effect of *at*RA on mitochondrial DNA copy number in three human hepatocyte donors. All experiments were conducted as described in the experimental section. Results are expressed as mean ± SD, n = 3. Comparisons between vehicle (ethanol) and *at*RA treated cells were made by Student's t-test: ***** indicates $p<0.05$ in comparison to vehicle treated controls.

Figure 4. The increase of mitochondrial biogenesis, fatty acid β-oxidation and ATP production by *at*RA treatment in HepG2 cells requires PPARδ. (A) The influence of RARα, RARβ and PPARδ siRNA on the induction of mitochondrial biogenesis genes by *at*RA. (B) The effect of RARβ and PPARδ siRNA on the induction of ATP production by *at*RA (C and D) The effect of RARβ and PPARδ siRNA on the induction of SDHA protein expression by *at*RA as measured by western blotting. Panel C shows the quantification of replicate western blots and panel D shows representative western blot. The representative blot shows analysis of biological duplicates for each treatment. Panels E and F show the effect of RARβ and PPARδ siRNA on fatty acid β-oxidation (E) and induction of mitochondrial DNA copy number (F) by *at*RA in HepG2 cells. Results for the mRNA, mitochondrial DNA, fatty acid oxidation and ATP

Molecular Pharmacology Fast Forward. Published on February 26, 2016 as DOI: 10.1124/mol.116.103697
This article has not been copyedited and formatted. The final version may differ from this version.

production studies are presented as fold change compared to vehicle (ethanol). Results for protein studies are presented as ratio of target protein over loading control β-Actin. Results are expressed as mean ± SD, n = 3. ***** indicates $p<0.05$ in comparison to the vehicle. # indicates $p<0.05$ in comparison to the scrambled siRNA plus *at*RA treated group.

Figure 5. *at*RA increases mitochondrial biogenesis and ATP production in lipid loaded HepG2 cells and human hepatocytes. (A) Oil Red O staining of control treated and lipid loaded HepG2 cells. Oil Red O staining was measured by quantifying the absorbance at 492 nM wavelength. The measured OD value for vehicle treated cells was 1.203 and for oleic acid loaded cells 2.642. (B) Induction of the mRNA expression of key mitochondrial biogenesis genes (PGC1α, PGC1β and NRF1) by *at*RA, talarozole or their combination in the lipid loaded HepG2 cells. (C) Induction of ATP production by *at*RA, talarozole or their combination in lipid loaded HepG2 cells. (D) Induction of SDHA protein expression following treatment of lipid loaded HepG2 cells with *at*RA as measured by western blotting. The quantification of the replicate western blots and a representative blot of triplicate treatments is shown. (E) Induction of the mRNA expression of key mitochondrial biogenesis genes by 1 μM *at*RA in lipid loaded human hepatocytes from three individual donors. (F) Induction of ATP production by 1 μM *at*RA in lipid loaded human hepatocytes from three individual donors. Results for mRNA studies are presented as fold change in mRNA abundance relative to vehicle (ethanol). mRNA results, ATP assay and protein expression results are expressed as mean ± SD, n = 3. Comparisons between vehicle (ethanol) and *at*RA treated cells were made by Student's t-test: *****, $p<0.05$ versus vehicle. #, $p<0.05$ versus 1 μM *at*RA. †, $p<0.05$ versus 100nM *at*RA.

Molecular Pharmacology Fast Forward. Published on February 26, 2016 as DOI: 10.1124/mol.116.103697
This article has not been copyedited and formatted. The final version may differ from this version.

Figure 6. *at*RA requires PPARδ in the regulation of mitochondrial biogenesis in lipid loaded HepG2 cells. (A) The induction of nuclear receptor mRNA by 1 μM *at*RA in lipid loaded HepG2 cells. (B) The influence of RARα siRNA on the induction of mitochondrial biogenesis genes by *at*RA. (C) The influence of RARβ siRNA on the induction of mitochondrial biogenesis genes. (D) The influence of PPARδ siRNA on the induction of mitochondrial biogenesis genes. Results are presented as fold change in mRNA abundance relative to vehicle (ethanol). mRNA results are expressed as mean ± SD, n = 3 and are representative of at least 3 separate studies. *****, $p<0.05$ versus vehicle. #, $p<0.05$ versus scrambled plus *at*RA.

Figure 7. Effect of *at*RA and talarozole treatment on mitochondrial biogenesis markers and fatty acid oxidation genes in vivo in mice. (A) Hepatic mRNA expression of Pgc1α, Pgc1β, Nrf, Atgl and Cpt1α in mice treated with *at*RA. (B) Quantification of mitochondrial DNA in *at*RA and vehicle treated mice following an overnight fast (fasted group) or 4 hours later following feeding. (C and D) Induction of liver SDHA protein expression in *at*RA and vehicle treated mice as measured by western blotting. Panel C shows the quantification of the western blots and panel D shows the representative blot image. The blot shows analysis of three individual mice for each treatment. (E) Hepatic mRNA expression of Rarβ and Cyp26a1 in *at*RA or vehicle treated mice (F) Induction of hepatic mitochondrial biogenesis genes in mice following talarozole treatment in comparison to vehicle treated mice. All mRNA data are presented as fold change in mRNA abundance relative to control mice. β-Actin was used as the housekeeping gene. For protein data, results are expressed as ratio of SDHA to β-Actin. Results are expressed as mean ± SD, n = 4. Comparisons between control fasted and *at*RA fasted, and vehicle and TLZ were made by Student's t-test: *****, $p<0.05$ versus vehicle or control.

Molecular Pharmacology Fast Forward. Published on February 26, 2016 as DOI: 10.1124/mol.116.103697
This article has not been copyedited and formatted. The final version may differ from this version.

Figure 8. Mitochondrial biogenesis and fatty acid oxidation pathways induced by *at*RA in the liver models and a proposed molecular mechanism for the observed effects. (A) Collective representation of fatty acid metabolism and mitochondrial function proteins and mRNA which were induced by *at*RA in the models of human liver. Green boxes and circles indicate proteins and mRNA that were shown to increase in expression in response to *at*RA treatment. (B) Proposed molecular mechanism of *at*RA regulation of mitochondrial function.

Molecular Pharmacology Fast Forward. Published on February 26, 2016 as DOI: 10.1124/mol.116.103697
This article has not been copyedited and formatted. The final version may differ from this version.

Tables

Table 1: Relative proteomic analysis of the effects of *at*RA on protein expression in HepG2 cells. The changes were quantified via spectral counting. Significant differences are underlined. Only proteins for which the same peptide was consistently detected in all replicate control and treated samples are shown.

	UniProt ID	RA/Con	p-value	Protein Name	Gene Name
Transcription	Q92804	1.00	1.00	TATA-binding protein-associated factor 2N	TAF15
	P12004	0.93	0.23	Proliferating cell nuclear antigen	PCNA
	P20290	1.21	0.02	Transcription factor BTF3	BTF3
	Q13185	0.88	0.02	Chromobox protein homolog 3	CBX3
	Q08211	1.51	0.04	ATP-dependent RNA helicase A	DHX9
RNA Processing	O43776	1.15	0.33	Asparagine--tRNA ligase, cytoplasmic	NARS
	Q99714	0.63	0.15	3-hydroxyacyl-CoA dehydrogenase type-2	HSD17B10
	O75643	1.70	0.004	U5 small nuclear ribonucleoprotein 200 kDa helicase	SNRNP200
	P31942	1.91	0.008	Heterogeneous nuclear ribonucleoprotein H3	HNRNPH3
	Q1KMD3	1.36	0.01	Heterogeneous nuclear ribonucleoprotein U-like protein 2	HNRNPUL2
	P55795	0.70	0.01	Heterogeneous nuclear ribonucleoprotein H2	HNRNPH2
	P23246	1.20	0.03	Splicing factor, proline- and glutamine-rich	SFPQ
	Q16630	1.30	0.03	Cleavage and polyadenylation specificity factor subunit 6	CPSF6
	P49588	1.32	0.03	Alanine--tRNA ligase, cytoplasmic	AARS
	Q15637	1.40	0.04	Splicing factor 1	SF1
Translation	P46779	0.52	0.01	60S ribosomal protein L28	RPL28
	P56537	0.96	0.77	Eukaryotic translation initiation factor 6	EIF6
	P62241	0.80	0.02	40S ribosomal protein S8	RPS8
	Q9NR30	1.32	0.01	Nucleolar RNA helicase 2	DDX21
	P24534	1.28	0.02	Elongation factor 1-beta	EEF1B2
	P26373	0.73	0.03	60S ribosomal protein L13	RPL13
Protien integrity	P61604	0.78	0.27	10 kDa heat shock protein, mitochondrial	HSPE1
	Q9Y3C6	0.95	0.42	Peptidyl-prolyl cis-trans isomerase-like 1	PPIL1
	P13667	1.18	0.02	Protein disulfide-isomerase A4	PDIA4
	P27797	1.24	0.03	Calreticulin	CALR
	P08107	2.70	0.03	Heat shock 70 kDa protein 1A/1B	HSPA1A
	Q9Y4L1	1.50	0.03	Hypoxia up-regulated protein 1	HYOU1
	P11021	0.93	0.04	78 kDa glucose-regulated protein	HSPA5
	P08238	1.13	0.04	Heat shock protein HSP 90-beta	HSP90AB1
Protease activity	P49720	0.90	0.69	Proteasome subunit beta type-3	PSMB3
	Q99436	0.75	0.29	Proteasome subunit beta type-7	PSMB7
	P35998	1.20	0.02	26S protease regulatory subunit 7	PSMC2
	P55036	1.21	0.04	26S proteasome non-ATPase regulatory subunit 4	PSMD4
ar tra ffic	Q9Y678	0.85	0.11	Coatomer subunit gamma-1	COPG1

Molecular Pharmacology Fast Forward. Published on February 26, 2016 as DOI: 10.1124/mol.116.103697
This article has not been copyedited and formatted. The final version may differ from this version.

	Q8TEX9	1.28	0.03	Importin-4	IPO4
	Q14974	1.15	0.004	Importin subunit beta-1	KPNB1
	P51149	1.37	0.03	Ras-related protein Rab-7a	RAB7A
	O00151	1.30	0.04	PDZ and LIM domain protein 1	PDLIM1
Metabolism	P23526	1.05	0.59	Adenosylhomocysteinase	AHCY
	O60701	0.93	0.16	UDP-glucose 6-dehydrogenase	UGDH
	P51659	1.30	0.49	Peroxisomal multifunctional enzyme type 2	HSD17B4
	P40925	1.01	0.72	Malate dehydrogenase, cytoplasmic	MDH1
	Q15181	1.22	0.26	Inorganic pyrophosphatase	PPA1
	Q9NR45	0.98	0.89	Sialic acid synthase	NANS
	O43175	1.03	0.53	D-3-phosphoglycerate dehydrogenase	PHGDH
	Q8NF37	1.00	1.00	Lysophosphatidylcholine acyltransferase 1	LPCAT1
	P54819	1.03	0.64	Adenylate kinase 2, mitochondrial	AK2
	Q06830	1.02	0.685	Peroxiredoxin-1	PRDX1
	P14324	1.52	0.01	Farnesyl pyrophosphate synthase	FDPS
	Q99541	2.57	0.001	Perilipin-1	PLIN2
	P49327	1.27	0.002	Fatty acid synthase	FASN
	P06737	2.46	0.00	Glycogen Phosphorylase, liver form	PYGL
	Q13011	1.27	0.006	Delta(3,5)-Delta(2,4)-dienoyl-CoA isomerase, mitochondrial	ECH1
	Q95573	1.56	0.01	Long-chain-fatty-acid-CoA ligase 3	ACSL3
	P17174	2.11	0.01	Aspartate aminotransferase, cytoplasmic	GOT1
	P49419	1.74	0.01	Alpha-aminoadipic semialdehyde dehydrogenase	ALDH7A1
	Q86SX6	2.26	0.01	Glutaredoexin-related protein 5, mitochondrial	GLRX5
	P12268	1.50	0.01	Inosine-5'-monophosphate dehydrogenase 2	IMPDH2
	Q53HR2	1.68	0.01	Acyl-Coenzyme A dehydrogenase	ACAD
	P25705	1.56	0.02	ATP synthase subunit alpha, mitochondrial	ATP5A1
	Q8NBX0	1.35	0.02	Saccharopine dehydrogenase-like oxidoreductase	SCCPDH
	O60448	1.38	0.02	Long-chain-fatty-acid-CoA ligase 4	ACSL4
	P05091	1.24	0.03	Aldehyde dehydrogenase, mitochondrial	ALDH2
	P48735	1.67	0.03	Isocitrate dehydrogenase [NADP], mitochondrial	IDH2
	P51648	1.88	0.03	Fatty aldehyde dehydrogenase	ALDH3A2
	P52209	1.44	0.03	6-phosphogluconate dehydrogenase, decarboxylating	PGD
	P00387	1.29	0.03	NADH-cytochrome b5 reductase 3	CYB5R3
	P12277	1.38	0.04	Creatine kinase B- type	CKB
	P80404	2.00	0.04	4-aminobutyrate aminotransferase, mitochondrial	ABAT
	P78417	1.34	0.04	Glutathione S-transferase omega-1	GSTO1
	P50897	1.62	0.04	Palmitoyl-protein thioesterase 1	PPT1
	P11586	1.28	0.04	C-1-tetrahydrofolate synthase, cytoplasmic	MTHFD1
Cell cycle regulation	P42166	0.85	0.67	Thymopoietin isoform alpha	TMPO
	P33991	1.45	0.13	DNA replication licensing factor MCM4	MCM4
	P33993	0.94	0.67	DNA replication licensing factor MCM7	MCM7

Molecular Pharmacology Fast Forward. Published on February 26, 2016 as DOI: 10.1124/mol.116.103697
This article has not been copyedited and formatted. The final version may differ from this version.

	P49736	1.47	0.004	DNA replication licensing factor MCM2	MCM2
	P62826	1.14	0.04	GTP-binding nuclear protein Ran	RAN
	P18754	1.35	0.01	Regulator of chromosome condensation	RCC1
Cell survival	O75874	1.20	0.08	Isocitrate dehydrogenase [NADP] cytoplasmic	IDH1
	P38646	1.21	0.04	Stress-70 protein, mitochondrial	HSPA9
	Q13442	1.78	0.01	28 kDa heat- and acid-stable phosphoprotein	PDAP1
Apoptosis	P10599	1.00	1.00	Thioredoxin	TXN
	P21796	1.28	0.01	Voltage-dependent anion-selective channel protein 1	VDAC1
	P09382	0.95	0.64	Galectin-1	LGALS1
	Q9Y265	1.00	1.00	RuvB-like 1	RUVBL1
Structural integrity	P15924	0.93	0.28	Desmoplakin	DSP
	Q09666	1.64	0.19	Neuroblast differentiation-associated protein AHNAK	AHNAK
	Q15149	0.85	0.32	Plectin	PLEC
	Q01082	1.02	0.89	Spectrin beta chain	SPTBN1
	P63313	0.72	0.10	Thymosin beta-10	TMSB10
	Q9Y2B0	1.09	0.39	Protein canopy homolog 2	CNPY2
	P35579	2.61	0.02	Myosin-9	MYH9
	P67936	2.58	0.01	Tropomyosin alpha-4 chain	TPM4
Misc.	P08758	1.12	0.31	Annexin A5	ANXA5
	Q13283	1.19	0.41	Ras GTPase-activating protein-binding protein 1	G3BP1
	Q96CN7	0.72	0.23	Isochorismatase domain-containing protein 1	ISOC1
	Q9H3K6	1.38	0.30	BolA-like protein 2	BOLA2

Molecular Pharmacology Fast Forward. Published on February 26, 2016 as DOI: 10.1124/mol.116.103697
This article has not been copyedited and formatted. The final version may differ from this version.

Table 2: Cell media *at*RA, 4-OH-*at*RA and 4-oxo-*at*RA concentrations at the end of the 24 hour treatment with vehicle, *at*RA, talarozole or the combination of *at*RA and talarozole.

Treatment	***at*RA (nM)**	**4-OH-*at*RA (nM)**	**4-oxo-*at*RA (nM)**
Vehicle (Ethanol)	0	0	0
*at*RA (1 μM)	129 ± 19	7.5 ± 1.2	7.4 ± 1.2
Talarozole (1 μM)	0	0	0
*at*RA (1 μM) + Talarozole (1 μM)	334.3 ± 26.8	0	1.5 ± 0.1

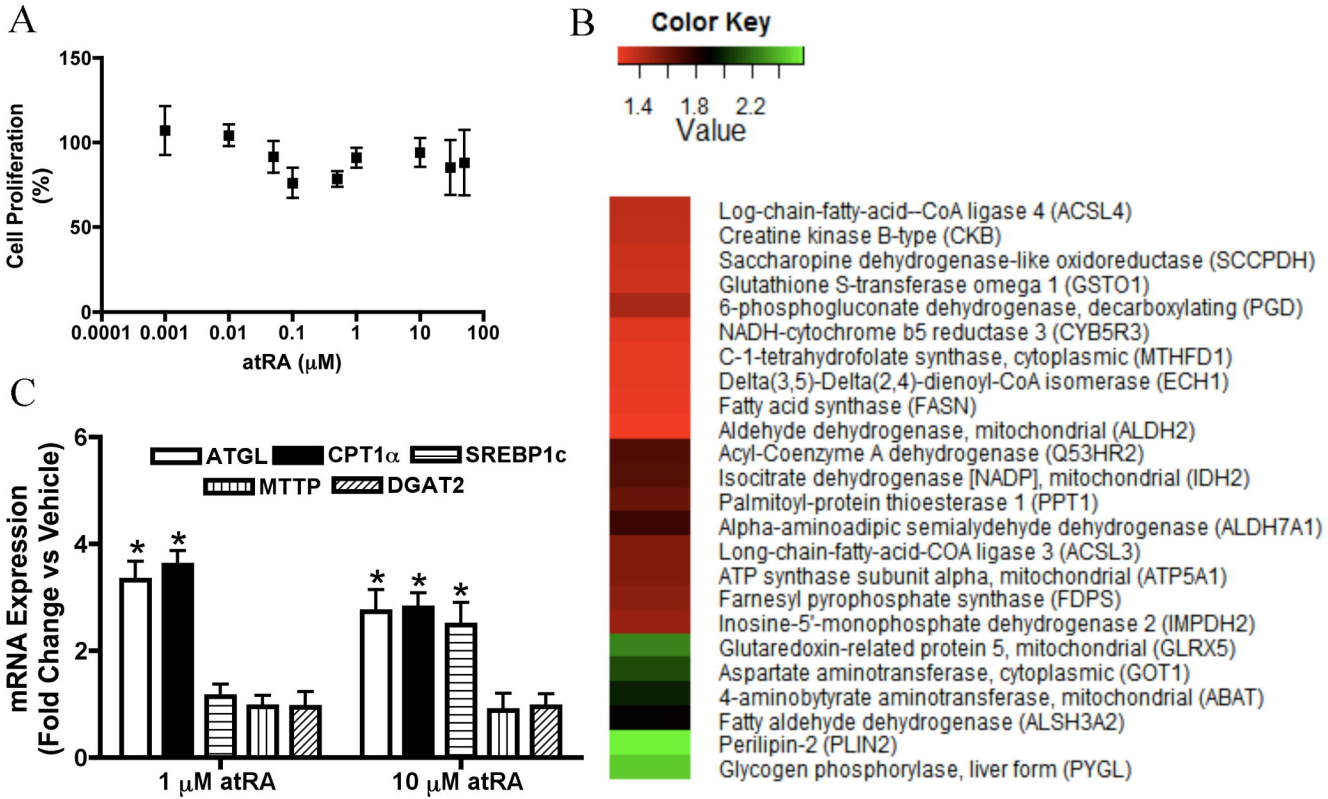
A
Cell Proliferation (%)
150
100
50
0
0.0001 0.001 0.01 0.1 1 10 100
atRA (μM)
B
Color Key
1.4 1.8 2.2
Value
Log-chain-fatty-acid--CoA ligase 4 (ACSL4)
Creatine kinase B-type (CKB)
Saccharopine dehydrogenase-like oxidoreductase (SCCPDH)
Glutathione S-transferase omega 1 (GSTO1)
6-phosphogluconate dehydrogenase, decarboxylating (PGD)
NADH-cytochrome b5 reductase 3 (CYB5R3)
C-1-tetrahydrofolate synthase, cytoplasmic (MTHFD1)
Delta(3,5)-Delta(2,4)-dienoyl-CoA isomerase (ECH1)
Fatty acid synthase (FASN)
Aldehyde dehydrogenase, mitochondrial (ALDH2)
Acyl-Coenzyme A dehydrogenase (Q53HR2)
Isocitrate dehydrogenase [NADP], mitochondrial (IDH2)
Palmitoyl-protein thioesterase 1 (PPT1)
Alpha-aminoadipic semialydehyde dehydrogenase (ALDH7A1)
Long-chain-fatty-acid-COA ligase 3 (ACSL3)
ATP synthase subunit alpha, mitochondrial (ATP5A1)
Farnesyl pyrophosphate synthase (FDPS)
Inosine-5'-monophosphate dehydrogenase 2 (IMPDH2)
Glutaredoxin-related protein 5, mitochondrial (GLRX5)
Aspartate aminotransferase, cytoplasmic (GOT1)
4-aminobytyrate aminotransferase, mitochondrial (ABAT)
Fatty aldehyde dehydrogenase (ALSH3A2)
Perilipin-2 (PLIN2)
Glycogen phosphorylase, liver form (PYGL)
C
mRNA Expression (Fold Change vs Vehicle)
6
4
2
0
ATGL
CPT1α
SREBP1c
MTTP
DGAT2
*
1 μM atRA
10 μM atRA

Figure 1

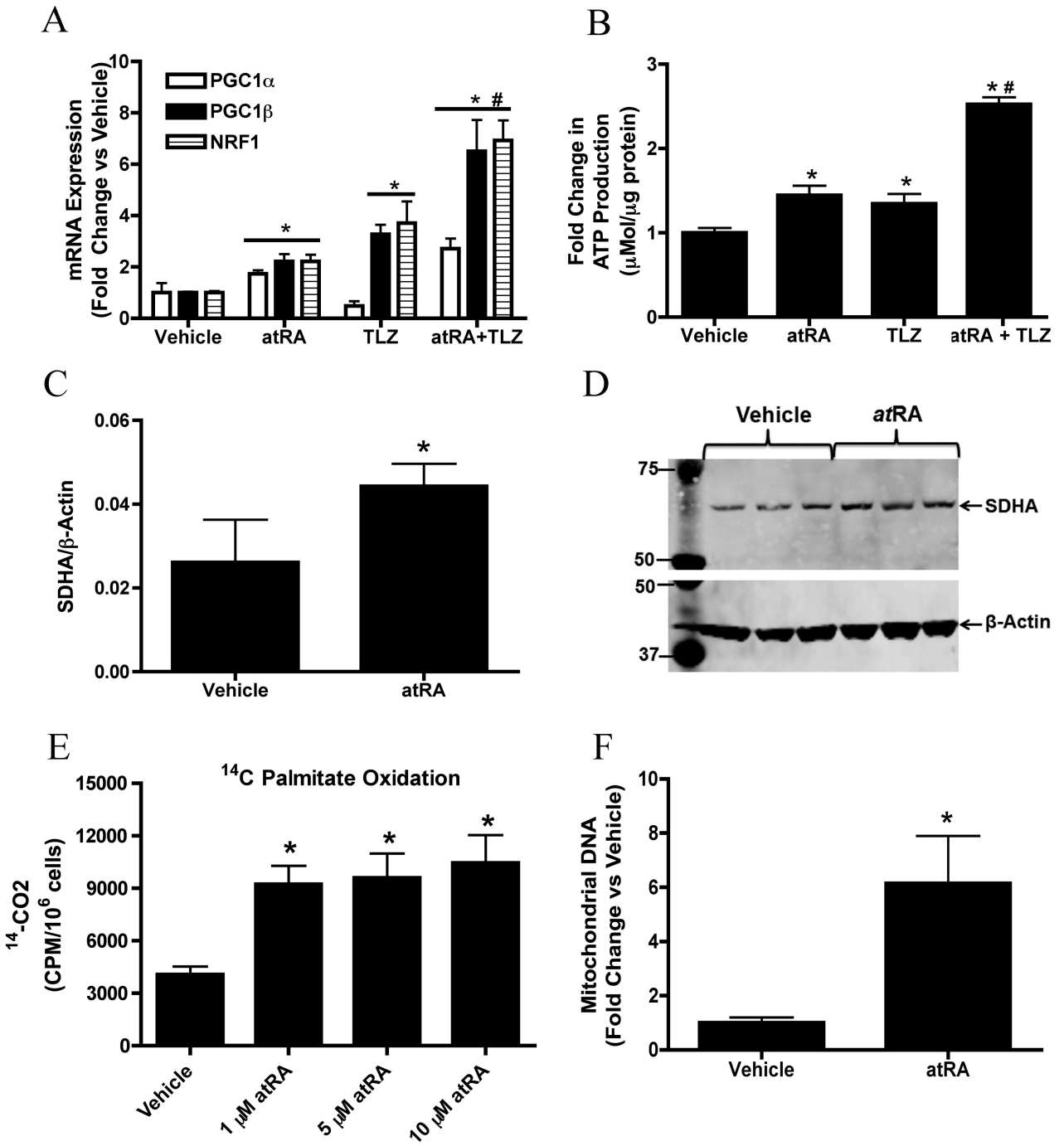
A
mRNA Expression (Fold Change vs Vehicle)
PGC1α
PGC1β
NRF1
Vehicle
atRA
TLZ
atRA+TLZ
B
Fold Change in ATP Production (μMol/μg protein)
Vehicle
atRA
TLZ
atRA + TLZ
C
SDHA/β-Actin
Vehicle
atRA
D
Vehicle
atRA
75
50
50
37
SDHA
β-Actin
E
14C Palmitate Oxidation
14-CO2 (CPM/10^6 cells)
Vehicle
1 μM atRA
5 μM atRA
10 μM atRA
F
Mitochondrial DNA (Fold Change vs Vehicle)
Vehicle
atRA

Figure 2

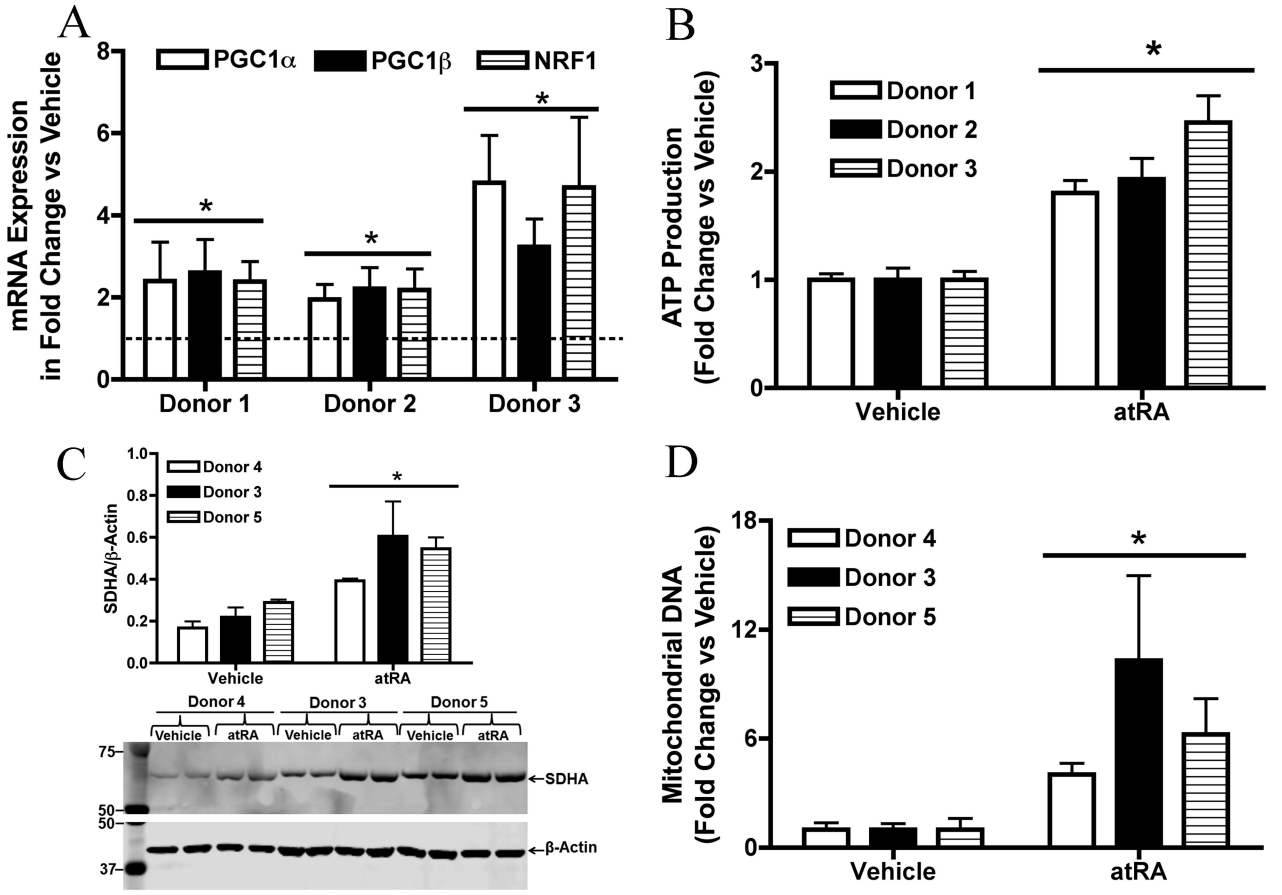
A
mRNA Expression in Fold Change vs Vehicle
PGC1α
PGC1β
NRF1
Donor 1
Donor 2
Donor 3
B
ATP Production (Fold Change vs Vehicle)
Donor 1
Donor 2
Donor 3
Vehicle
atRA
C
SDHA/β-Actin
Donor 4
Donor 3
Donor 5
Vehicle
atRA
SDHA
β-Actin
D
Mitochondrial DNA (Fold Change vs Vehicle)
Donor 4
Donor 3
Donor 5
Vehicle
atRA

Figure 3

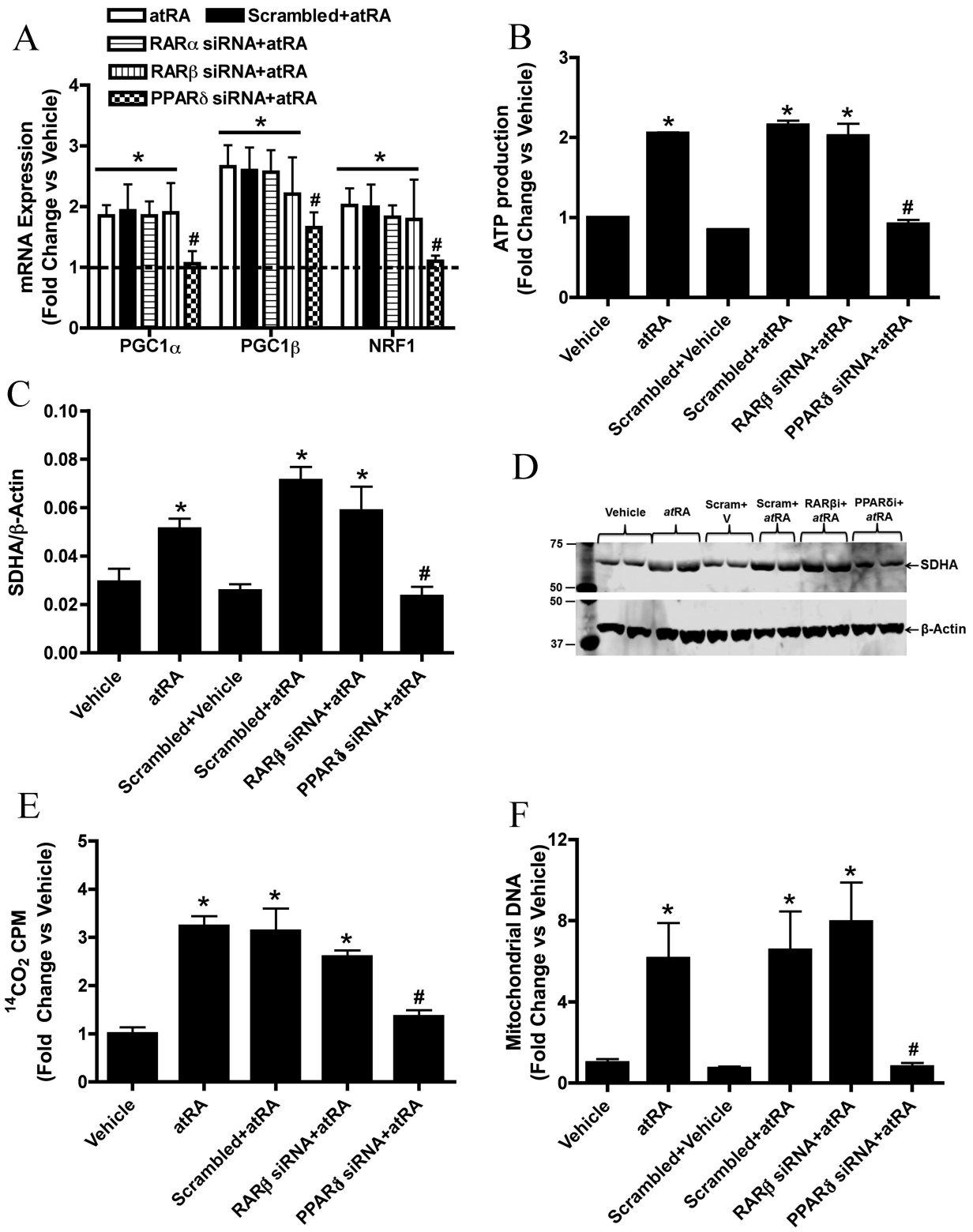
A
atRA
Scrambled+atRA
RARα siRNA+atRA
RARβ siRNA+atRA
PPARδ siRNA+atRA
mRNA Expression (Fold Change vs Vehicle)
PGC1α
PGC1β
NRF1
B
ATP production (Fold Change vs Vehicle)
Vehicle
atRA
Scrambled+Vehicle
Scrambled+atRA
RARβ siRNA+atRA
PPARδ siRNA+atRA
C
SDHA/β-Actin
D
Vehicle
atRA
Scram+ V
Scram+ atRA
RARβi+ atRA
PPARδi+ atRA
75
50
50
37
SDHA
β-Actin
E
14CO2 CPM (Fold Change vs Vehicle)
F
Mitochondrial DNA (Fold Change vs Vehicle)

Figure 4

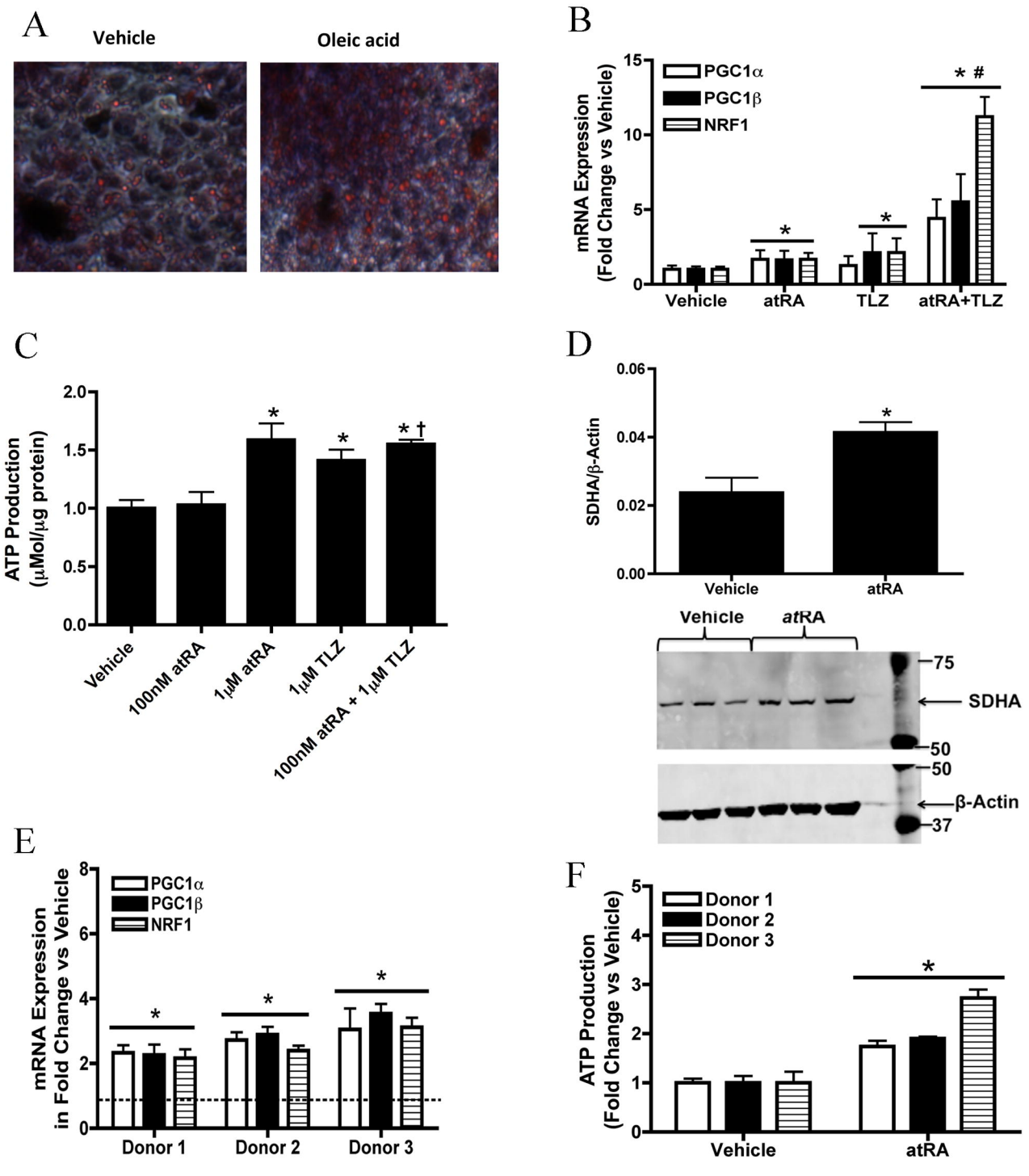
A
Vehicle
Oleic acid
B
PGC1α
PGC1β
NRF1
mRNA Expression (Fold Change vs Vehicle)
Vehicle
atRA
TLZ
atRA+TLZ
C
ATP Production (μMol/μg protein)
Vehicle
100nM atRA
1μM atRA
1μM TLZ
100nM atRA + 1μM TLZ
D
SDHA/β-Actin
Vehicle
atRA
SDHA
β-Actin
75
50
37
E
PGC1α
PGC1β
NRF1
mRNA Expression in Fold Change vs Vehicle
Donor 1
Donor 2
Donor 3
F
Donor 1
Donor 2
Donor 3
ATP Production (Fold Change vs Vehicle)
Vehicle
atRA

Figure 5

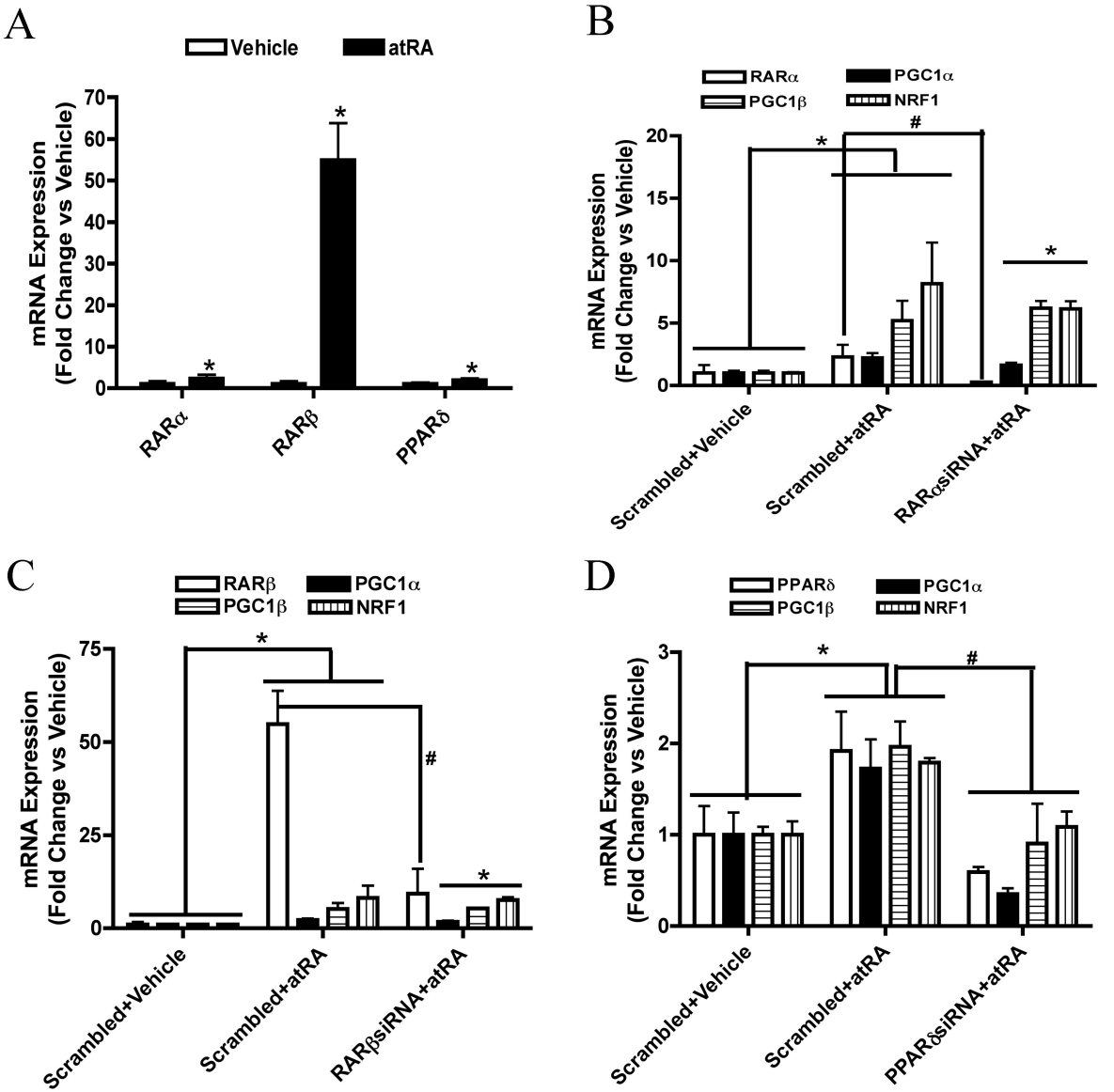
A
Vehicle
atRA
mRNA Expression
(Fold Change vs Vehicle)
70
60
50
40
30
20
10
0
*
*
*
RARα
RARβ
PPARδ
B
RARα
PGC1α
PGC1β
NRF1
mRNA Expression
(Fold Change vs Vehicle)
20
15
10
5
0
*
#
*
Scrambled+Vehicle
Scrambled+atRA
RARαsiRNA+atRA
C
RARβ
PGC1α
PGC1β
NRF1
mRNA Expression
(Fold Change vs Vehicle)
75
50
25
0
*
#
*
Scrambled+Vehicle
Scrambled+atRA
RARβsiRNA+atRA
D
PPARδ
PGC1α
PGC1β
NRF1
mRNA Expression
(Fold Change vs Vehicle)
3
2
1
0
*
#
Scrambled+Vehicle
Scrambled+atRA
PPARδsiRNA+atRA

Figure 6

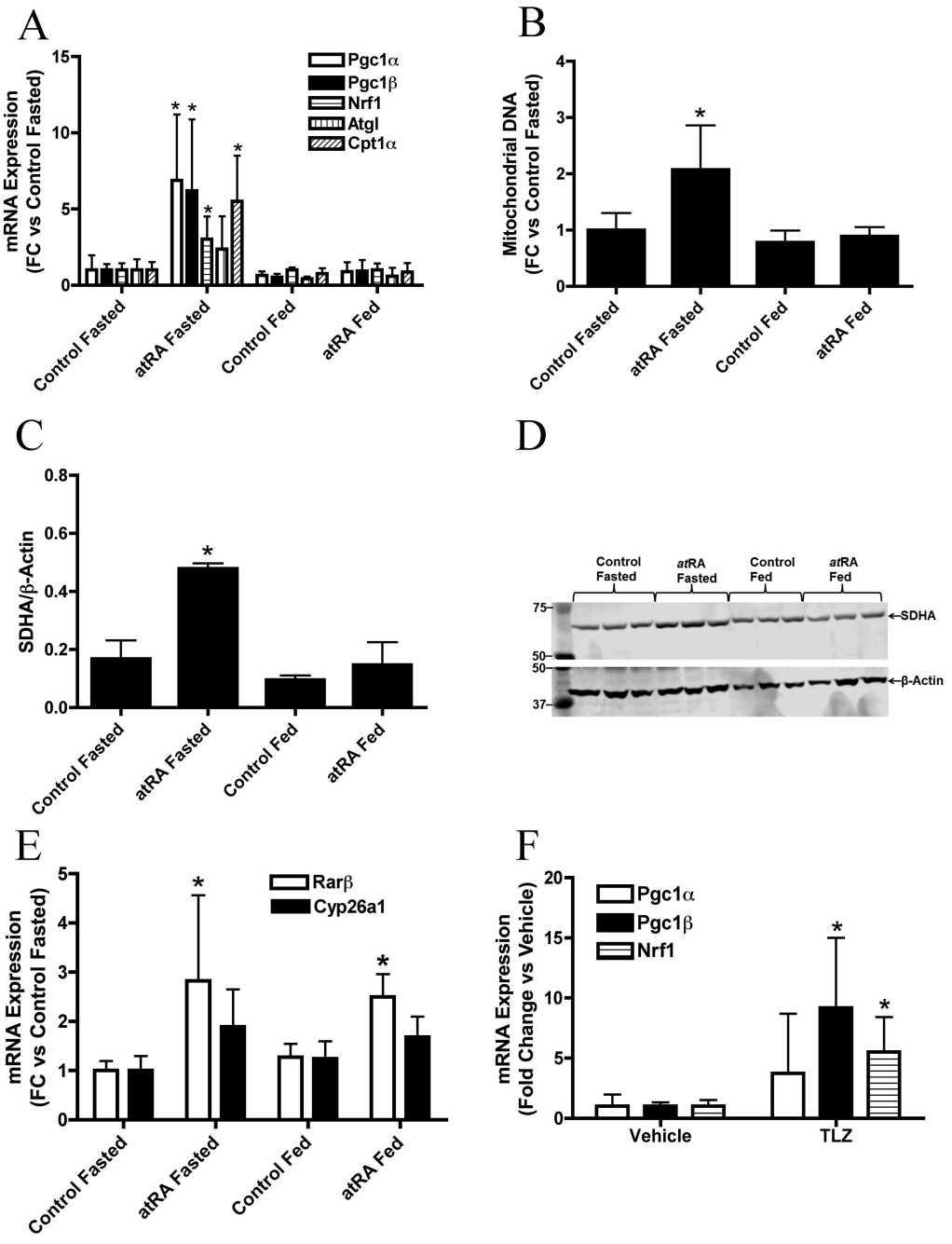
A
mRNA Expression
(FC vs Control Fasted)
Pgc1α
Pgc1β
Nrf1
Atgl
Cpt1α
Control Fasted
atRA Fasted
Control Fed
atRA Fed
B
Mitochondrial DNA
(FC vs Control Fasted)
C
SDHA/β-Actin
D
Control Fasted
atRA Fasted
Control Fed
atRA Fed
SDHA
β-Actin
E
mRNA Expression
(FC vs Control Fasted)
Rarβ
Cyp26a1
F
mRNA Expression
(Fold Change vs Vehicle)
Vehicle
TLZ

Figure 7

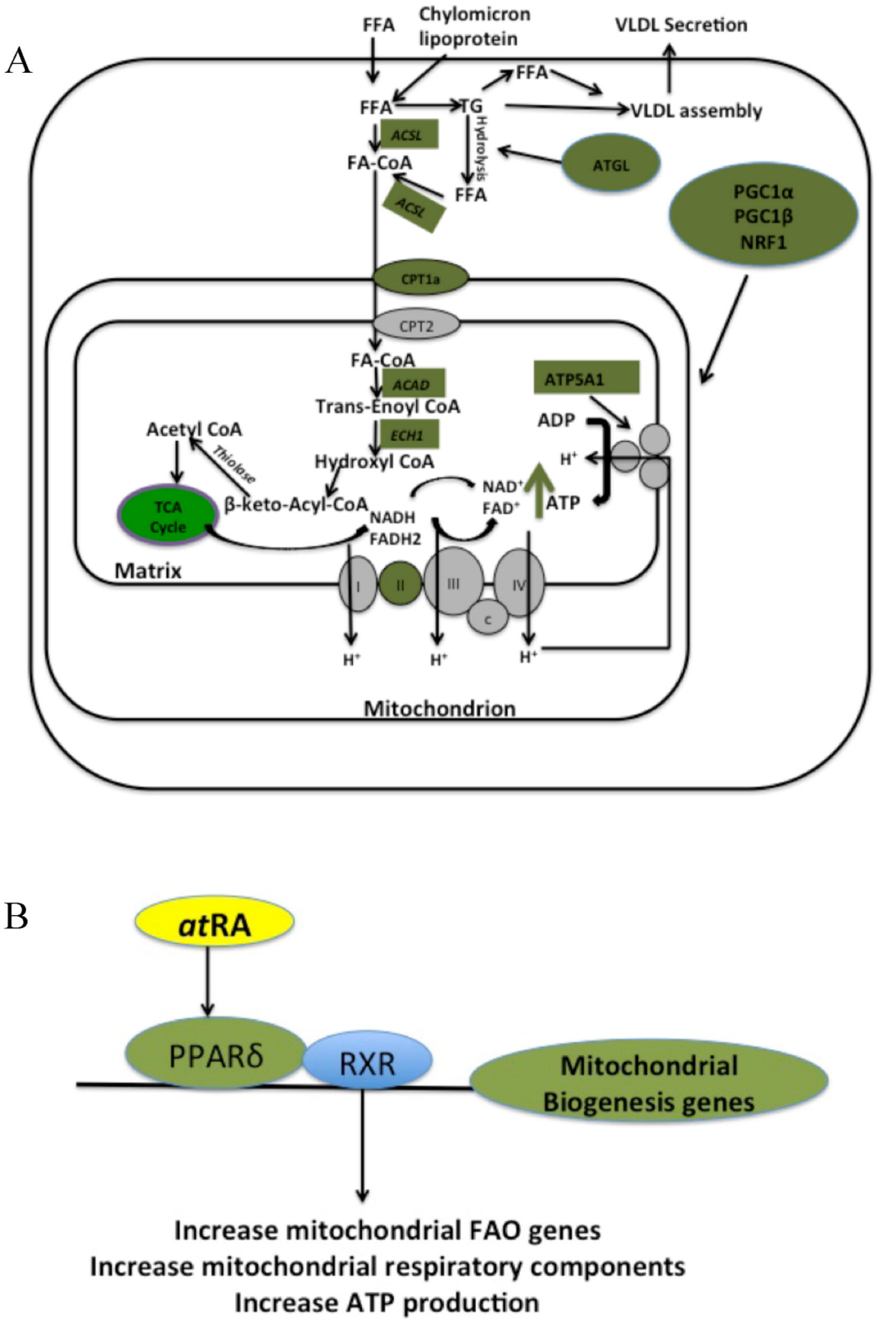
A
FFA
Chylomicron lipoprotein
VLDL Secretion
FFA
FFA
TG
VLDL assembly
ACSL
Hydrolysis
ATGL
FA-CoA
ACSL
FFA
PGC1α
PGC1β
NRF1
CPT1a
CPT2
FA-CoA
ACAD
ATP5A1
Trans-Enoyl CoA
ADP
Acetyl CoA
ECH1
H+
Thiolase
Hydroxyl CoA
NAD+
FAD+
ATP
TCA Cycle
β-keto-Acyl-CoA
NADH
FADH2
Matrix
I
II
III
IV
C
H+
H+
H+
Mitochondrion
B
atRA
PPARδ
RXR
Mitochondrial Biogenesis genes
Increase mitochondrial FAO genes
Increase mitochondrial respiratory components
Increase ATP production

Figure 8